



Regional correlation and seismic stratigraphy of Triassic Strata in the Greater Barents Sea: Implications for sediment transport in Arctic basins

Albina Gilmullina¹  | Tore Grane Klausen² | Niall William Paterson^{1,3} | Anna Suslova⁴ | Christian Haug Eide¹ 

¹University of Bergen, Bergen, Norway

²Petrolia NOCO AS, Bergen, Norway

³CASP, Madingley Rise, Cambridge, UK

⁴Lomonosov Moscow State University, Moscow, Russia

Correspondence

Albina Gilmullina, University of Bergen, Allégaten 41, Bergen, Norway.
Email: Albina.Gilmullina@uib.no

Funding information

Norges Forskningsråd, Grant/Award Number: 267689

Abstract

The Greater Barents Sea Basin (GBSB) in Arctic Russia and Norway is an intracratonic basin that accommodated an enormous amount of sediment during the Triassic. These deposits are up to 4.5 km thick over an area 2,500,000 km², and consist of marine mudstones and mudstone-rich fluvio-deltaic topsets with sandstone-dominated fluvial channels. The basin is well-studied and data-rich, but regional correlation between different parts is lacking. Provenance data from adjacent Arctic basins have been interpreted to imply sediment transport from the Ural orogen across the GBSB, but these are disputed because of great transport distances, poorly constrained sediment-transport directions and unknown timing of bypass. We integrated data from 3,238 seismic lines, 257 wells and palynostratigraphy, as well as published outcrop data, to create the first unified stratigraphic framework for the Triassic deposits across the entire GBSB. Results show that (1) sediment was transported northwest by one linked sedimentary system stretching across the entire basin; (2) sediment was derived from a source in the east comprising the Urals and West Siberia; (3) the main stratigraphic boundaries are major flooding surfaces which can be traced throughout the basin; and (4) significant amounts of sediment overspilled from the Barents Sea into adjacent sedimentary basins, starting with the Lomonosov Ridge from the Early Triassic, and into basins to the northwest (e.g. Sverdrup, Chukotka) during the late Carnian. These results provide a better understanding of geodynamics and provenance data in the Arctic, to improve the prediction of reservoirs in the area, and indicate a protracted uplift-history of the northernmost Urals that started in the Carnian ~237 Ma. Furthermore, it shows how large intracratonic basins interact with uplifts and subside over tens of millions of years.

KEYWORDS

Arctic, channels, cliniform, delta, large-scale basin infill, Svalbard, Triassic palynology

This is an open access article under the terms of the Creative Commons Attribution License, which permits use, distribution and reproduction in any medium, provided the original work is properly cited.

© 2020 The Authors. *Basin Research* published by International Association of Sedimentologists and European Association of Geoscientists and Engineers and John Wiley & Sons Ltd

1 | INTRODUCTION

The Greater Barents Sea Basin (GBSB, Figure 1) in Arctic Russia and Norway, was an enormous (c. 1,200 km EW, 1,800 km NS) sedimentary basin which accommodated a sedimentary succession up to 4.5 kilometres thick during Triassic (Glørstad-Clark et al., 2010; Henriksen, Ryseth, et al., 2011; Klausen et al., 2015; Norina et al., 2014). With an area of 2 500 000 km², the GBSB was about three times the size of the Northwestern Australian Shelf, five times the size of the North Sea and six times the size of the N Gulf of Mexico shelf. How such enormous sedimentary basins are filled by sediment through geological time has received little study, and in this contribution we integrate information from the entire GBSB to understand linkages between enormous basins and source-area geodynamics, and to better understand Triassic sediment routing in the Arctic basins.

The main tectonic driver that controlled sediment supply to the GBSB has been assumed to be regional contraction resulting in the Ural and Taimyr orogens east of the basin (Bergan & Knarud, 1993; Puchkov, 2009), but the emplacement of the Siberian Traps Large Igneous Province is also likely to have influenced sediment supply (cf. Reichow et al., 2009, Figure 1c). Analysis of GBSB basin fill provides insights into the longevity of topography and compression in the Urals, the effects of emplacement of the Siberian Traps Large Igneous Province, and the timing of the onset of uplift of the Novaya Zemlya Fold and Thrust Belt (NZFTB) and Pay-Khoy orogens in the northern Urals (Figure 1). The Barents and Kara seas are also believed to contain large amounts of hydrocarbon resources in the Triassic deposits and understanding the depositional history is critical to consider the location and timing of hydrocarbon formation (Artyushkov et al., 2014; Norwegian Petroleum Directorate Resource report, 2016, 2017; Stoupakova, 2011).

The GBSB has widespread and continuous Triassic deposits, and can be divided into six different geographic regions that will be referred to in this paper (Figure 1): (a) The Southwestern Barents Sea (Norwegian Barents Sea) and (b) Timan-Pechora Basin are well-explored areas, with abundant drilled wells and actively producing hydrocarbon fields; (c) The Eastern Barents Sea including Franz-Josef Land (Russian Barents Sea), which has limited coverage of seismic data and a limited number of exploration wells, (d) Northwestern Barents Sea, which has no active exploration but several research wells drilled and abundant 2D seismic data collected by the Norwegian Petroleum Directorate, (e) North Kara Sea, which currently has no wells and (f) the onshore areas of Svalbard, which offer widespread and accessible outcrops of Triassic deposits (e.g. Mørk et al., 1999; Mørk, Elvebakk, et al., 1999; Vigran et al., 2014).

The sediments filling in the GBSB originated mainly in the east (e.g. Artyushkov et al., 2014; Bergan & Knarud, 1993;

Highlights

- For the first time, the entire Triassic succession is correlated across the Greater Barents Sea Basin in Arctic Norway and Russia, and a common lithostratigraphic framework has been established for this enormous area that has seen little holistic study.
- Triassic sediments were dominantly supplied from source areas in the southeast which included both the Ural Orogen and West Siberia. This source was extremely productive, and created one sedimentary system that supplied mudstone-rich sediment which overspilled the Greater Barents Sea Basin, into adjacent basins in the Arctic towards the late Carnian and Norian.
- Local, more sand-rich and mineralogically mature deposits occur close to basement highs such as N Fennoscandia and Svalbard in the Early and Middle Triassic, but these become diluted or displaced by sediments from the East in the later Triassic.
- A three-stage depocentre shift is documented throughout the Triassic, and this is explained by geodynamic in the basins and source areas.
- Cretaceous igneous intrusions make up an essential part (c. 10%) of the Triassic succession in the Eastern Barents Sea, and this must be taken into account when investigating subsidence history of sedimentary basins.

Bue & Andresen, 2014; Eide et al., 2018; Fleming et al., 2016; Klausen et al., 2015; Mørk, Dallmann, et al., 1999; Mørk, Elvebakk, et al., 1999; Norina et al., 2014; Stoupakova, 2001). Thus, the Russian parts of the basin are proximal and the Norwegian parts of the basin are more distal. The sediments are composed of extensive mudstone-rich linked clinofor-delta-delta plain systems (e.g. Klausen & Mørk, 2014; Klausen et al., 2018, 2019) similar to other deltaic successions with continental-scale drainages, such as the Mississippi in the Gulf of Mexico (Blum & Pecha, 2014; Blum & Törnqvist, 2000; Galloway et al., 2011) and the Triassic Mungaroo Formation in the northwest Australia (e.g. Martin et al., 2018). The studied deltaic deposits are interspersed by regional flooding surfaces that serve as marker surfaces in the basin, enabling subdivision of the basin-fill into stratigraphic units (Dalland et al., 1988; Glørstad-Clark et al., 2010; Klausen et al., 2016; Mørk et al., 1989). Flooding surfaces coincide with boundaries in the biostratigraphic framework established for the

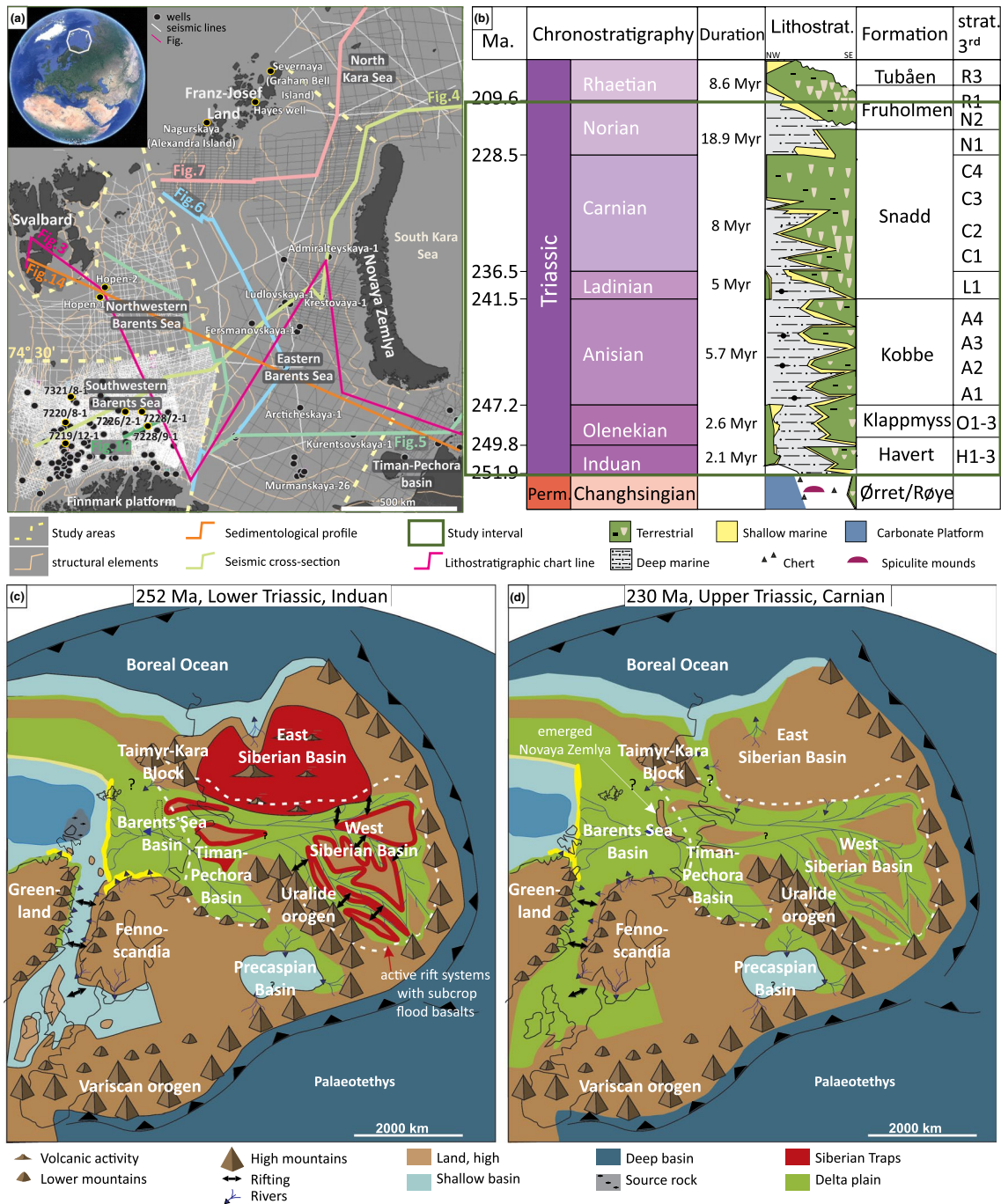


FIGURE 1 (a) Overview of the entire Greater Barents Sea Basin, the six geographic regions (see Introduction) and all seismic and well data available in this study. Structural elements modified from (Gabrielsen et al., 1990; Faleide et al., 2008). (b) Chronostratigraphic chart of the study interval and lithology of the well-studied SW Barents Sea (for more detailed description of stratigraphic units see Results). Modified from (Cohen et al., 2013; Eide et al., 2018; Gradstein et al., 2012; Klausen et al., 2016; Rossi et al., 2019). (c and d) Palaeogeographic map showing the regional setting of the study area in the early Induan (Early Triassic) and Carnian (Late Triassic). Based on a variety of sources, including (Nikishin et al., 2002; Cocks & Torsvik, 2006; Reichow et al., 2009; Nikishin et al., 2010; Miller et al., 2013; Sømme et al., 2018)

Western Barents sea (Paterson & Mangerud, 2020; Vigran et al., 2014; Figure 3) and are extended to the Eastern Barents sea of the study area using data from wells and seismic data across the GBSB (Figures 4 and 5), supported by published and re-analysed biostratigraphic data.

This paper has five goals: (a) To create a unified, cross-border stratigraphic framework for the large, easterly sedimentary system filling the Triassic Greater Barents Sea Basin, (b) to map the Triassic formations and their thicknesses in all available seismic and well data across the entire basin, (c) to

Age (Ma)/ Stage (Oggel et al., 2014)		Duration	Svalbard (Vigran et al., 2014)	Franz-Josef Land (Dymov et al., 2011)	Norwegian Barents Sea (Mørk et al., 1999; Gjørstad-Clark et al., 2010; Vigran et al., 2014; Klausen et al., 2015; Eide et al., 2018; Paterson et al., 2019; Rossi et al., 2019)	Russian Barents Sea (Fefilova, 2001; Repin et al., 2007)	Novaya Zemlya (Ustritsky, 1981; Cherkesov and Makarov, 1982; Fefilova, 2015)	Timan-Pechora (Morakhovskaya, 2000; Kirichkova et al., 2016)					
TRIASSIC	Late	Norian Rn.	Knorringsfjellet Formation Flatsalen Formation Slotlet Bed	Vasil'evskaya	Fruholmen Fm.	R2	Ludlovskaya	eroded					
				Heysovskaya		N2			Л Т _{3п} (L)	eroded			
				De Geerdalen Formation Tschermafjellet Formation		S6			K T _{3п} (K)		eroded		
						Gream-Bellskaya						N1	И Т _{2к} (E)
												S5	
	S4	C3	3 Т ₂₋₃ (Z)										
	Middle	Anisian Ladinian		Bravaisberget Formation Botneheia Formation	Ermakovskaya	Kobbe Fm.	C2	Arcticheskaya	Anguranskaya				
			Matusevichskaya		L1		Ж Т _{2л} (Zh)			Nar'yanmarkaya			
					Belozemelskaya						A4	E T _{2а-1} (Ye)	Korotaihkinskaya
			A3				Д Т _{2а} (D)			Nyadeyinskaya			
A2													
A1													
Early	Olenekian Induan	Villingodden Formation Vikinghøgda Formation Vardebukta Formation	Belozemelskaya	Klappmyss Fm.	O3	Admiralteyskaya (Sedoyakhskaya) red-colored rocks	Kharaleyskaya						
					Sassendalen Gr.			S2	Г Т _{1о} (G)	Lestanshorskaya			
								Havert Fm.	O2		B T _{1о-2} (V)		
					O1				Б Т _{1о} (B)				
					S1				H3	A ₂ T _{1л2} (A ₂)	Charkabozhskaya		
H2	A ₂ T _{1л-2} (A ₂)	hiatus											
H1	A ₁ T _{1л} (A ₁)												

Western source

Southern source

South-Eastern source

FIGURE 2 Comparison of formation and sequence subdivisions in different basins. Colours marked different sources that engaged on sedimentation of marked formations. Light green—Greenland, pink—Fennoscadian shield and blue—Ural, Taimyr, West Siberia and Siberian traps

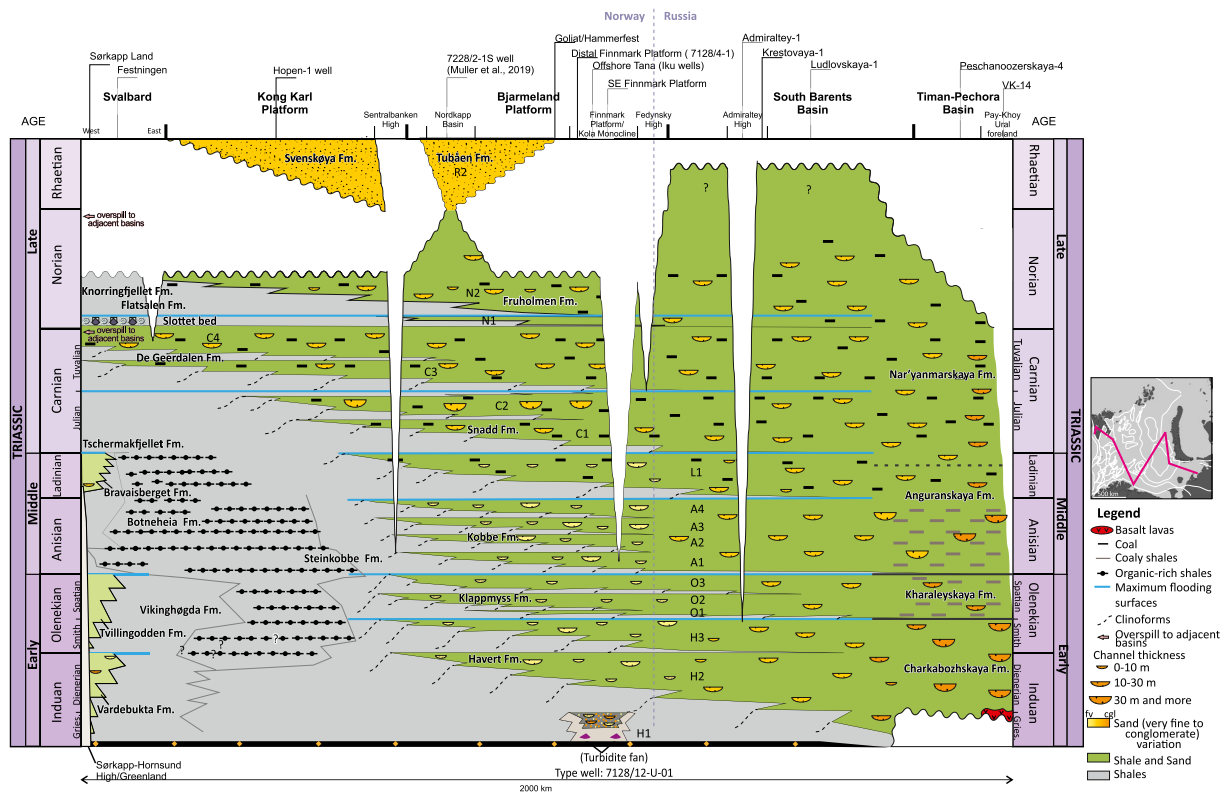


FIGURE 3 Lithostratigraphic correlation of the Triassic between different parts of the Greater Barents Sea Basin, for location see Figure 1, after (Eide et al., 2018; Fefilova, 2013b; Klausen et al., 2015; Krajewski & Weitschat, 2015; Morakhovskaya, 2000; Mørk, Dallmann, et al., 1999; Mørk, Elvebakk, et al., 1999; Mørk & Worsley, 2006; Norina et al., 2014; Rossi et al., 2019; Stoupakova et al., 2011)

present palynological data that for the first time illustrates the Russian assemblages and verifies the seismic interpretations across the GBSB, (d) to understand how Triassic sediments were distributed and how different parts of the basin were interlinked and (e) provide a framework to understand the growing provenance database in the Triassic Arctic. Together these have important implications on palaeogeographic reconstructions and petroleum prospectivity in the region.

2 | GEOLOGICAL SETTING

2.1 | Basin evolution

In the Western Barents Sea basin, the basement is overlain by post-Caledonian sedimentary rocks, and is shallow compared to the basement in the Eastern Barents Sea (Faleide et al., 1984): generally the depth to basement is c. 8 km but beneath localised salt basins it may reach up to 12 km (Aarseth et al., 2017). In the Eastern Barents Sea, the basement is generally overlain by post-Cambrian sediments (Stoupakova, 2011) and located at up to 20 km depth (Gac et al., 2012). In the western Barents Sea, northeast striking rift basins contain mobile salt, and these developed during Late Devonian–mid-Carboniferous rifting (Gudlaugsson et al., 1998). After post-Caledonian rifting ended in the Late Devonian (Eastern Barents Sea) and Carboniferous (Western Barents Sea), the Western Barents Sea subsided slowly and was infilled with carbonates and mudstones until the latest Permian (e.g. Gac et al., 2014; Worsley, 2008). In the Eastern Barents Sea, the transition from carbonates to siliciclastic deposits happened earlier, during the Artinskian (early Permian), because of supply of clastic sediments from the Ural Orogen (Ustritsky & Tugarova, 2013). Rapid and poorly understood subsidence of the entire GBSB occurred from the start of the Triassic (e.g. Clark et al., 2014).

2.2 | Sediment sources and surrounding uplands

The Ural orogen (Figures 1c and 2) is traditionally regarded as the main sediment source for the Triassic of the GBSB (e.g. Bergan & Knarud et al., 1993; Flowerdew et al., 2020; Mørk, Dallmann, et al., 1999; Mørk et al., 1999). The Ural orogen is a result of a continent–continent collision between Laurussia and Kazahkstania in the Mississippian–Lopingian, and later with Siberia in the Polar Urals, and the Pay-Khoy-Novozemelian foldbelt in the Late Triassic and Early Jurassic (Puchkov, 2009). In the Permian, the foreland basin close to the Ural orogen filled with siliciclastic deposits, but carbonate and spiculite sedimentation dominated in the West and central parts of the GBSB (Worsley, 2008), showing that subsidence

balanced sediment supply during the main orogenic phase. Subsequently, during the Induan, large amounts of sediments prograded into the GBSB from the East (Figure 3) (e.g. Eide et al., 2018; Glørstad-Clark et al., 2010). It is worth pointing out that the most significant phases of compression in the Urals occurred during the Carboniferous to early Permian, with waning tectonism and relief into the Permian and Triassic (Puchkov, 2009), and that the rapid progradation in the Induan happened at a time where large-scale compression in the Uralian orogeny is not expected. The Induan progradation coincides with extensive volcanic activity in the Siberian Traps Large Igneous Province in West Siberia (e.g. Burgess & Bowring, 2015), and it is likely that tectonic uplift of the Urals, Taimyr and West Siberia occurred because of magmatic activity (Puchkov, 2010; Sobolev et al., 2009) and led to the widespread progradation of sedimentary system in the Triassic. The Taimyr orogen (Figure 1c,d), located northeast of the Novaya Zemlya, has also been suggested as a sediment source that can explain differences in sandstone composition and zircon ages between the Southwestern Barents Sea and Svalbard (Fleming et al., 2016). The commonality for all the Eastern sediment sources (Urals, Taimyr, Siberian Traps) is that they provided relatively immature sandstones with abundant feldspar and volcanic fragments (Bergan & Knarud, 1993; Mørk, Dallmann, et al., 1999; Mørk, Elvebakk, et al., 1999), and a very large proportion of mud (e.g. Eide et al., 2018; Klausen et al., 2018).

Other minor sediment sources were the Fennoscandian Shield to the south, and Greenland (Figures 2 and 3) to the west of the GBSB during the Early until the beginning of Late Triassic; these provided more quartz-rich sands to areas close to the basin margins (e.g. Bue & Andresen, 2014; Eide et al., 2018; Mørk, Dallmann, et al., 1999; Mørk, Elvebakk, et al., 1999). The Novaya Zemlya and Pay-Khoy ranges could also have been important sediment sources, but only after these areas were uplifted during the latest Triassic and Early Jurassic (e.g. Drachev, 2016; Müller et al., 2019; Scott et al., 2010). However, the exact time of uplift of these areas is poorly dated.

2.3 | Post-depositional evolution

Overlying the Triassic succession, a regional unconformity is developed in the Western Barents Sea (Figure 3), likely caused by contraction-related uplift of Novaya Zemlya (Müller et al., 2019). This unconformity is expressed as an erosive contact between the Triassic and the overlying Rhaetian to Lower–Middle Jurassic deposits. Meanwhile, in the Eastern Barents Sea, an Early Jurassic foreland basin developed in front of the Novaya Zemlya fold-and-thrust belt (e.g. Olausen et al., 2018; Scott et al., 2010), which reached a thickness of up to 1.2 km (Suslova, 2014).

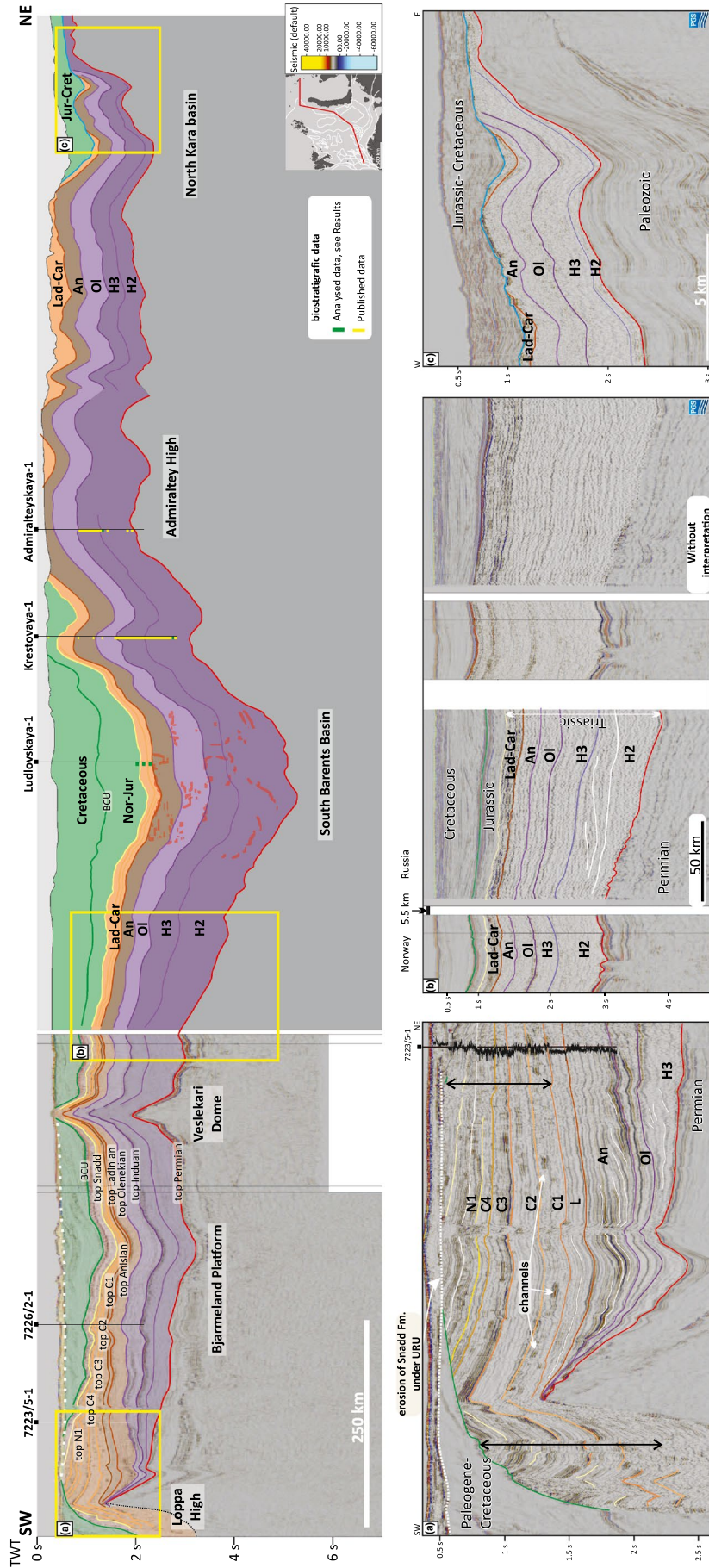


FIGURE 4 A regional composite seismic line from the Loppa High via the Admiralteyskaya-1 to the Kara Sea, showing the typical character of the Triassic deposits in the GBSB. Note the tabular seismic units over a very large area. (a) Overview with the most important well penetrations. (b) The westernmost extent of studied seismic data. Note the clearly expressed clinoforms, the downlap of the Induan to Anisian deposits onto the Loppa High, the drowning of the Loppa High in the Anisian, the clearly expressed discontinuous reflections in the topsets (fluvial channel deposits) and the erosion thickening and erosion below the Quaternary deposits of the Carnian unit. (c) Seismic data from the formerly disputed zone to the Eastern Barents Sea Basin. Note the well-expressed stratigraphic boundaries (based on well-imaged regional flooding surfaces), the similarity of deposits on both sides of the 5.5 km gap between the Norwegian and Russian data and the clearly expressed igneous intrusions in the east. (d) Seismic data of the most proximal parts of the Kara sea. Note the gradual onlap of the angular unconformity below the Triassic deposits and the clearly expressed Induan deposits onto this unconformity and the truncation of Triassic deposits below the Base Jurassic Unconformity

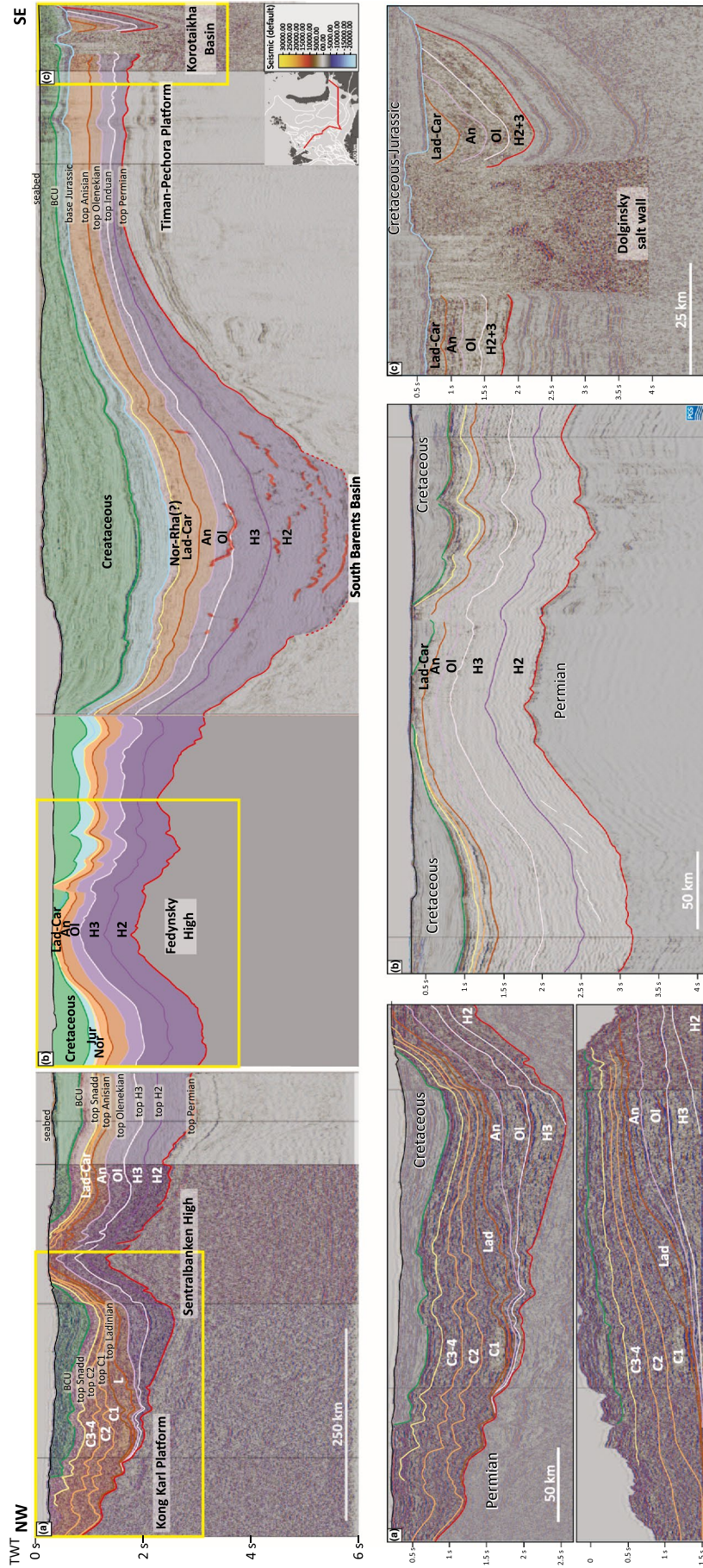


FIGURE 5 A regional composite seismic line from the Svalbard platform to the Korotaiikha Basin. Note A) the extreme thickness of the Induan compared to the rest of the deposits in the South Barents Basin and the extreme thickness of the Camian deposits in the Kong Karl platform, how tabular the stratigraphic units are, and the fact that nearly all geometric variations are caused by post-depositional tectonics, indicating that the Triassic was a structurally quiescent time in the basin; bright reflectors in the South Barents Sea are Cretaceous intrusions. Yellow box A) Unflattened (upper) and flattened (lower) on Permian–Triassic boundary the northwestmost seismic line shows progradation on unit L, C1–4; box B) the Lower and Middle Triassic strata without any thickness changes on the Fedyinsky High, the upper part of the Upper Triassic eroded by URU; box C) Triassic strata tilted by a salt wall in the western part of Korotaiikha Basin, where the easternmost strata tilted due to Pay-Khoy–Novaya Zemlya fold and thrust belt, also note an angular unconformity on top of the Triassic

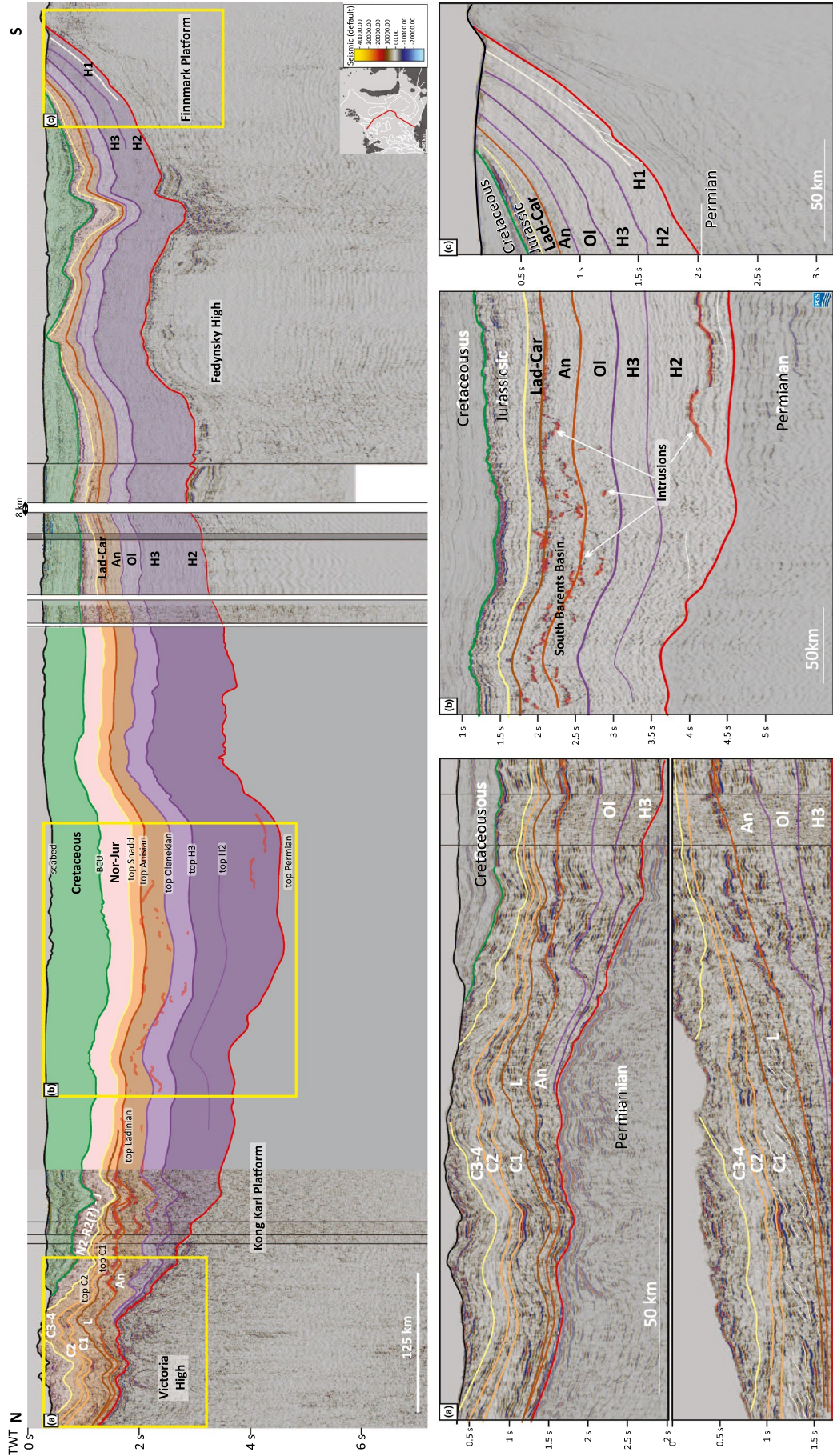


FIGURE 6 A regional composite seismic line from the Finnmark platform in the south and the Victoria High on the north. Note A) the same progradational Carnian units in the north as they are shown in Figure 5; (B) Triassic strata are hosting two types of Cretaceous intrusions—clinoform shape in unit H2 and saucer-shaped in Olenekian and Anisian units. C) Also note the H1 unit in the south, which is the only observable sedimentary unit from Fennoscandia, the rest of the Triassic deposits are sourced from the East

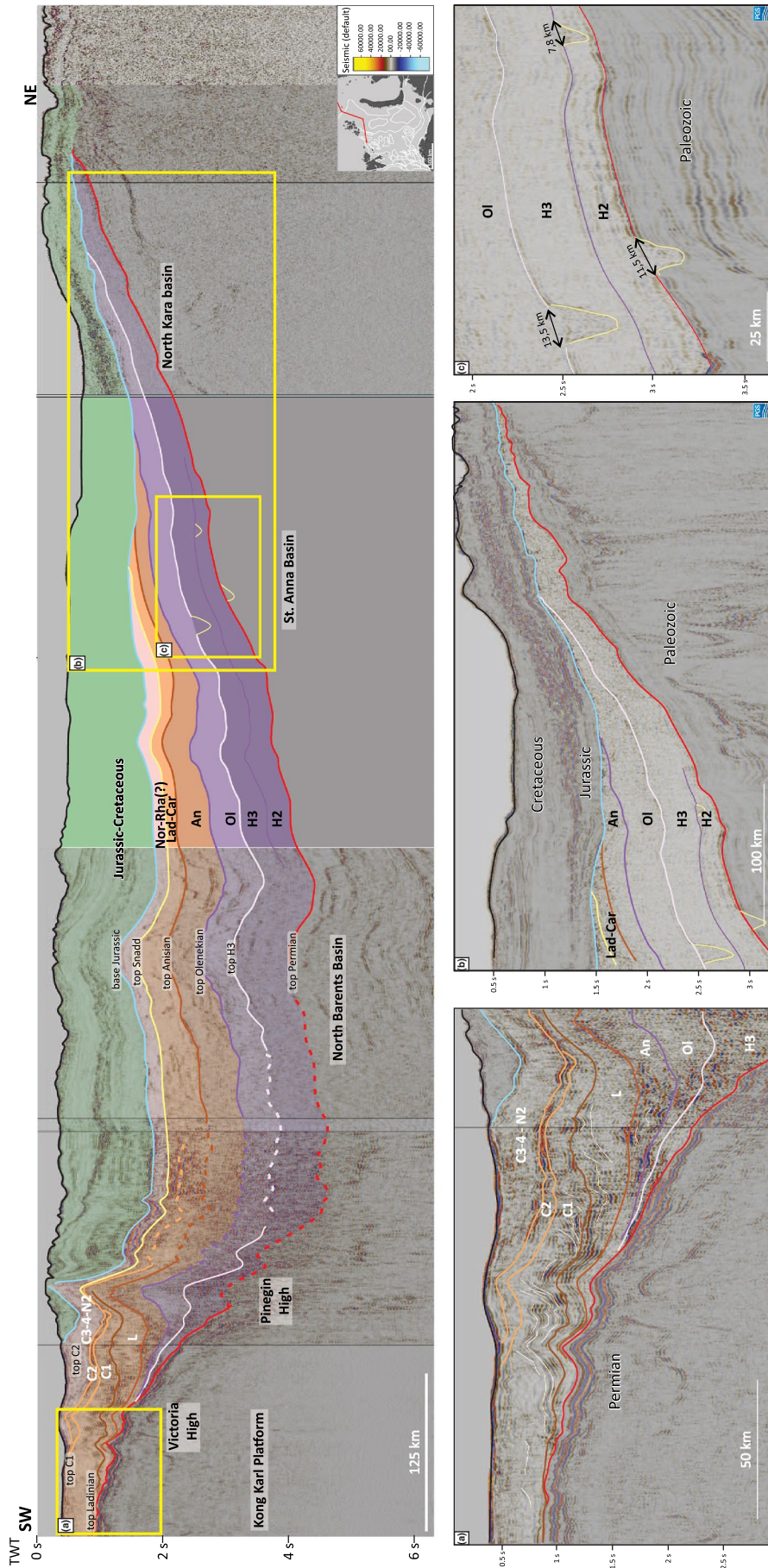


FIGURE 7 A regional composite seismic line in the northern part of the study area from the Kong Karl platform to North Kara Basin. Note A) the overview line shows the same structure with the thickest Lower Triassic in the central part and thinning towards the west. B) Although, the Triassic strata relatively thin towards the north, they remain continuous, were eroded by T/J unconformity. C) bottoms of units H2, H3 and Olenekian contain valley-shape erosive features

The GBSB was later buried beneath kilometres of Cretaceous deposits (Figure 6). During the Lower Cretaceous the High Arctic Large Igneous Province (HALIP) developed, and a vast quantity of magma intruded the sedimentary succession in the Northern and Eastern Barents Sea (Figures 4–7) (Polteau et al., 2016). During Atlantic breakup in the Paleogene, the Barents Sea was affected by compressional movements leading to the uplift of Svalbard, Novaya Zemlya and the Central Barents Sea (Henriksen, Bjørnseth, et al., 2011). During the Cenozoic, the basin has mainly been under uplift and erosion,

and erosion varies from c. 2.5 km on Svalbard and Novaya Zemlya (Figures 4 and 7), to c. 1.5 km in the Southwestern Barents Sea, and c. 400 m in the Eastern Barents Sea Basin (Figure 8) (Henriksen, Bjørnseth, et al., 2011).

2.4 | Palynological studies

Palynological data are critical in large-scale stratigraphic correlation because it provides (1) relative datings on sedimentary

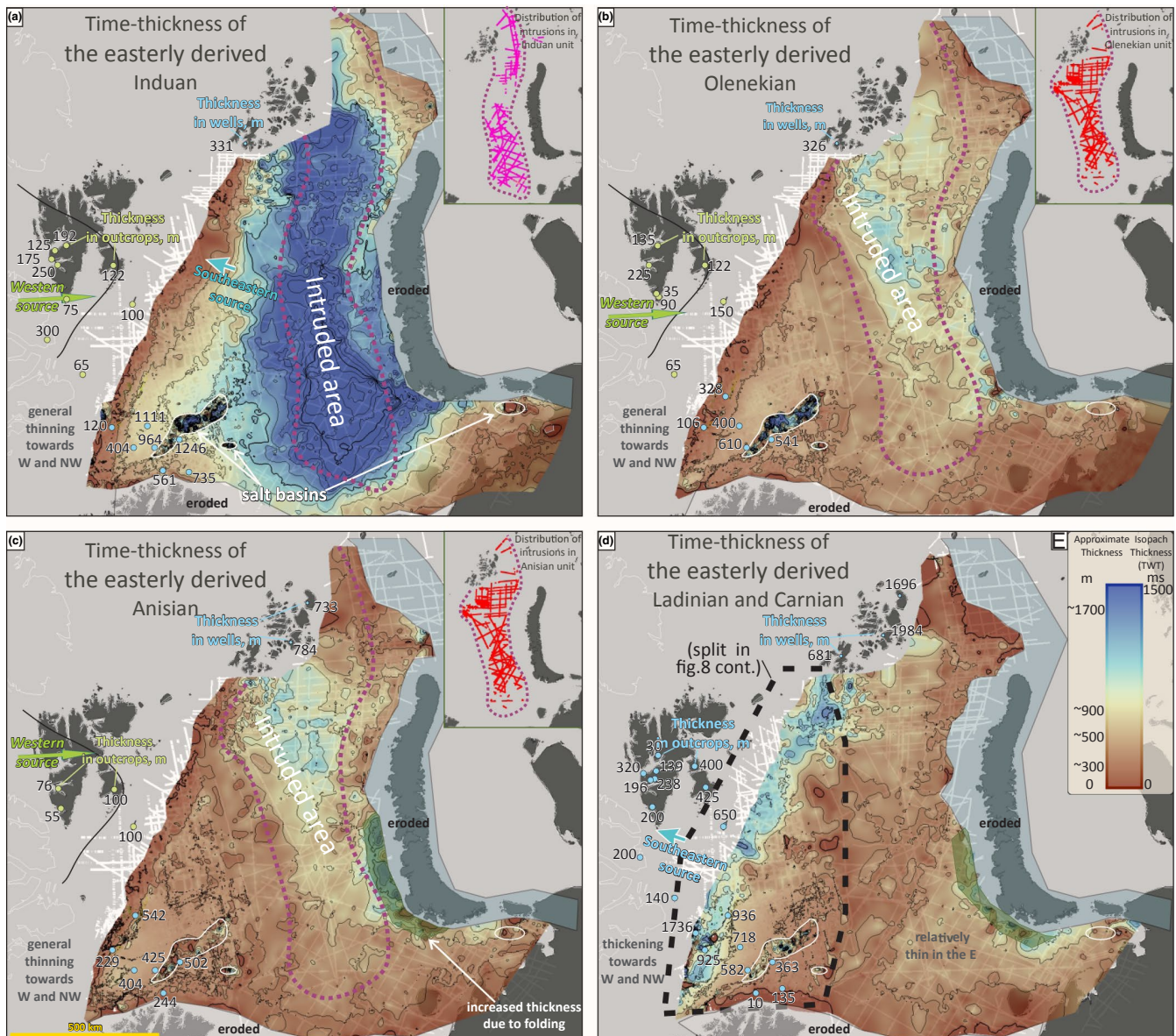


FIGURE 8 Time-thickness maps for the main stratigraphic units, colour scale equal for the different maps. (A) Induan; (B) Olenekian; (C) Anisian; (D) Ladinian-early Norian. Inset shows the location of igneous intrusions in each unit. The colour scale from (Crameri, 2018). Thickness maps of the Ladinian (F) and Carnian (G–I) deposits. Note the gradual progradation towards Svalbard. Location of clinoforms-concordant intrusions (K-i), saucer-shaped intrusions (K-ii) and seismically imaged dykes (K-iii) related to the High Arctic Large Igneous Province, the map used from Minakov et al. (2018). Names on the map: AAM, Artic Alaska margin; AR, Alpha Ridge and tentative location of magmatic centre; AX, Axel Heiberg Island; BI, Bennett Island; CHB, Chukchi Borderland; EL, Ellesmere Island; FJL, Franz Josef Land; GRE, Greenland; KKL, Kong Karls Land; SV, Svalbard

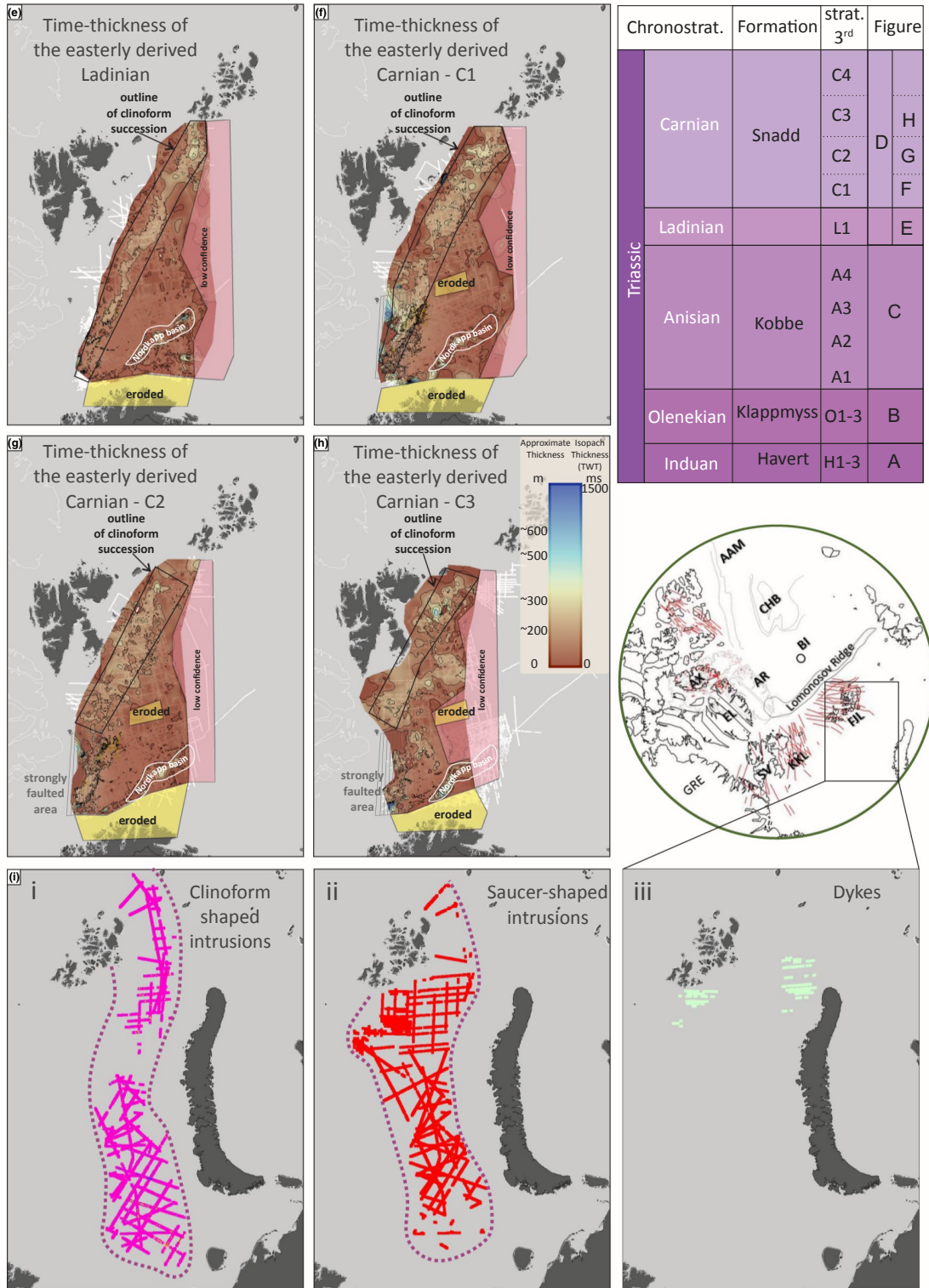


FIGURE 8 (Continued)

packages and the surfaces that bound them, (2) independent confirmation that stratigraphic packages correlate with each other and (3) enables stratigraphic subdivision of thick sedimentary packages without clearly traceable reflectors, such as the mainly alluvial late Triassic succession in the Eastern Barents

Sea. Palynostratigraphy thus provides independent verification of seismic interpretations, and stratigraphic subdivisions where no seismic subdivision is possible. This is important because seismic reflectors represent lithological changes that may, but do not necessarily have, chronostratigraphic significance

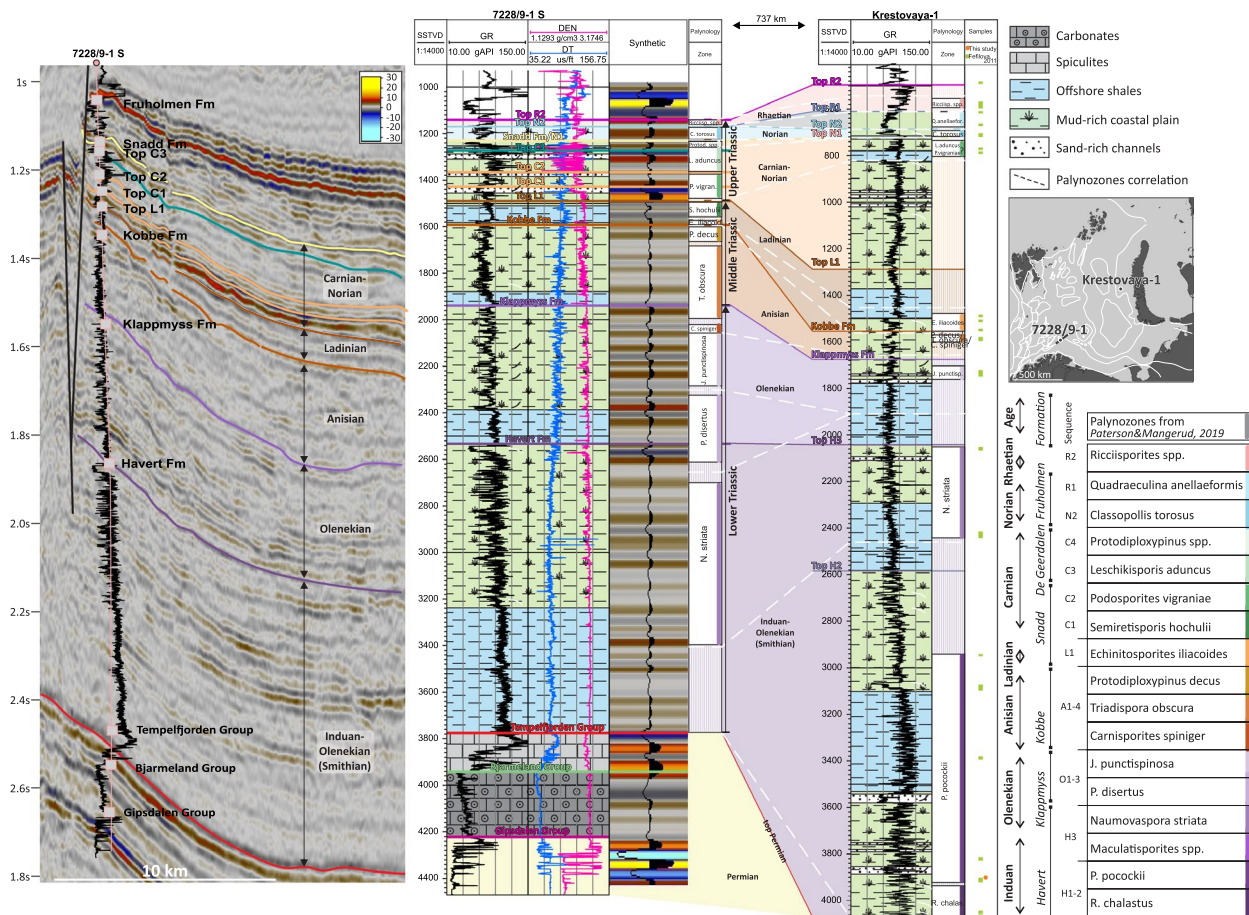


FIGURE 9 Interpretation and correlation of seismic, well-logs and biostratigraphic data penetrating the Triassic succession. Note the high gamma-ray values on the top of the low values, indicating maximum flooding surfaces and correlation boundaries across the basin. They might be found in Western and Eastern parts of the GBSB. Palynological zones for well 7228/9-1s after Paterson and Mangerud (2017) and Rossi et al. (2019). Palynological data from Krestovaya-1 after Fefilova (2013a), re-interpreted within the zonal framework of Vigran et al. (2014) and Paterson and Mangerud (2020)

across very large distances, and seismic interpretation can be challenging and not necessarily correct in areas that are deeply buried, structurally deformed or intruded.

Until now, no stratigraphic or palynological studies in the GBSB have been conducted with the objective to link the entire area. Rather, palynological studies have focused on smaller regions, such as Svalbard (Bjærke & Manum, 1977; Smith et al., 1975), the Norwegian Barents Sea and Svalbard (e.g. Hochuli et al., 1989; Paterson & Mangerud, 2020; Vigran et al., 2014) and the Russian Barents Sea (Fefilova, 2001, 2005, 2011, 2013a, 2013b; Klubov, 1965). Mørk et al. (1993) represent the only previous attempt to compare the respective palynofloras in the Norwegian and Russian parts of the Greater Barents Sea. Their work suggested clear differences in the ranges of palynomorph taxa between the two areas, something that would make correlations across the entire GBSB difficult. However, this difference may simply reflect differences in the taxonomic approach applied by different research groups. Currently, this has been difficult to assess

because here is a general lack of fundamental documentation of the Russian assemblages, such as an illustration of the age diagnostic palynomorphs taxa recorded. Such issues emphasise the need for holistic studies of the GBSB.

3 | METHODS AND DATA

3.1 | Seismic

The data coverage in the subsurface of the GBSB varies markedly between areas (Figure 1a). The average distance between individual 2D seismic lines are c 3 km in the Southwestern Barents Sea (several 3D seismic surveys are also available here), 14 km in the Northwestern Barents Sea, 125 km in the Eastern Barents Sea and 150 km in the Kara Sea.

This study is based on an analysis of 3,238 2D seismic lines covering 1,700,000 km², 257 wells with logs

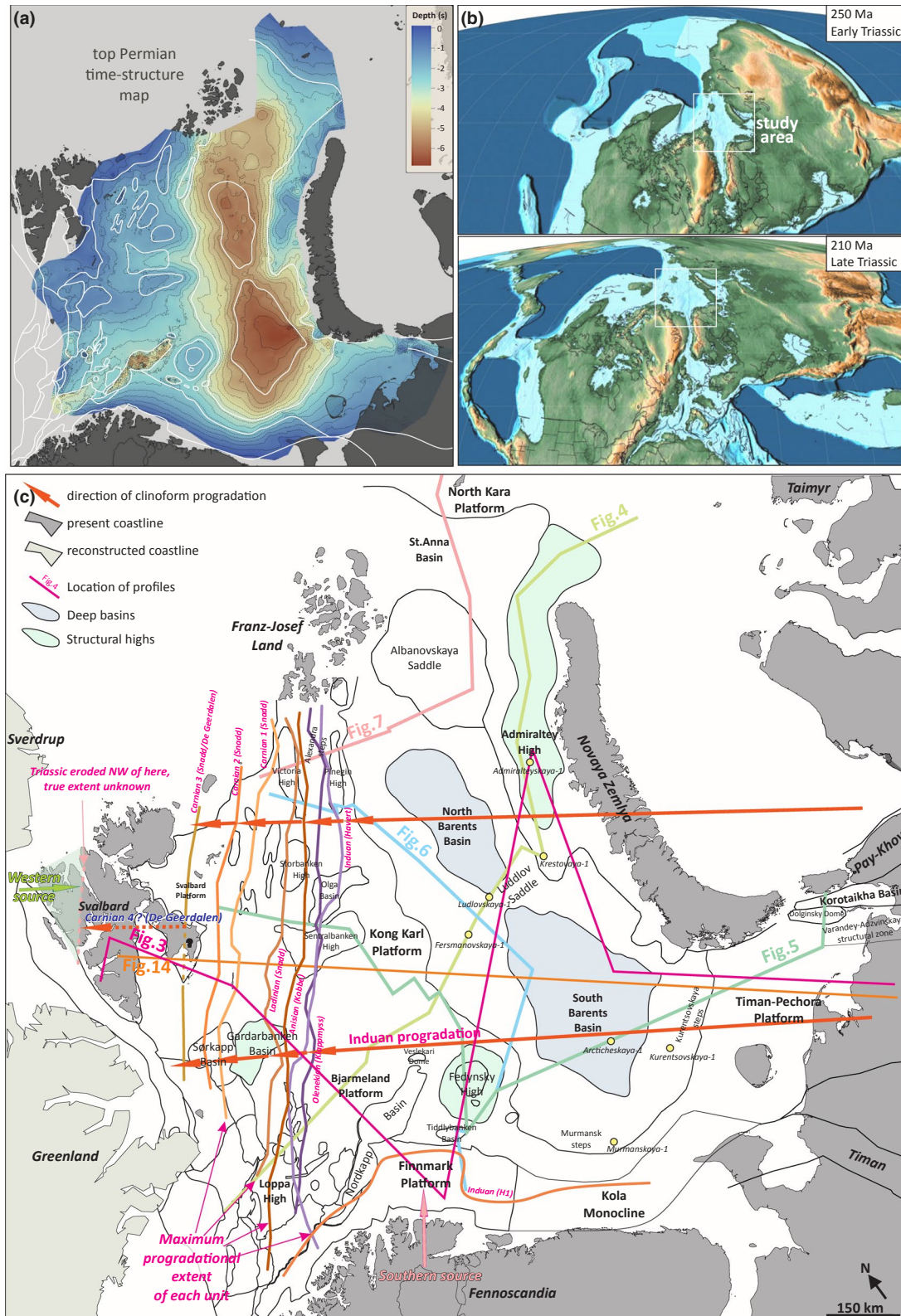


FIGURE 10 (a) Time-structural map of the base Triassic, (b) A regional overview of the GBSB location from (Scotese & Wright, 2018). (c) Maximum progradational extent of basinward clinoforms breaks in each studied time unit, and the observed progradation directions. Note the linear front of each clinoforms package, the consistent direction of sediment transport through time and the extreme progradational extent of the Induan package. H1 based on Eide et al., 2017 study, the location of Greenland and Sverdrup from (Shephard et al., 2013). Updated version of structural elements can be found in Supplementary materials (Supplement 2) as well as shelf-edge maximum progradation

and palynostratigraphic data. Six of the wells are from the Russian Barents Sea. The tops and bottoms of the different prograding seismic units were interpreted in the seismic and matched with constrained age in wells that become a basis for a definition of the thickness of studied units.

3.2 | Interpretation of stratigraphic units

Access to seismic data from the earlier disputed area between Norway and Russia (cf. Henriksen & Uflstein, 2011), provided by the Norwegian Petroleum Directorate, made it

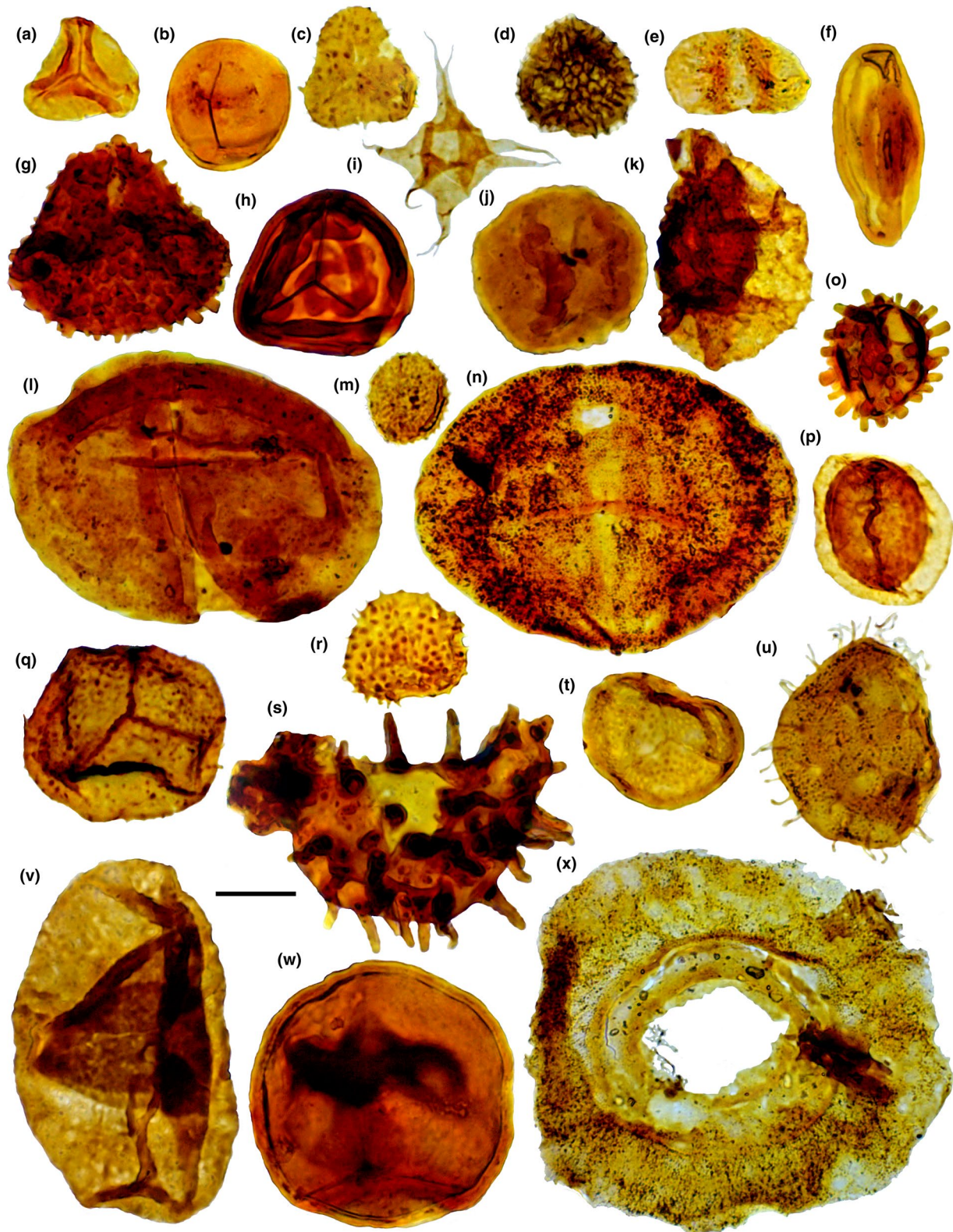


FIGURE 11 Early–Middle Triassic (Induan–Ladinian) palynomorph taxa from the Fersmanovskaya-1, Kurentsovskaya-1 and Murmanskaya-26 wells. Scale bar = 20µm. A. Dictyophyllidites mertonii, Kurentsovskaya-1, 2086–2097m; B. Leschikisporis aduncus, Murmanskaya-26, 2212.8 Early–Middle Triassic (Induan–Ladinian) palynomorph taxa from the Fersmanovskaya-1, Kurentsovskaya-1 and Murmanskaya-26 wells. Scale bar = 20µm. A. Dictyophyllidites mertonii, KurentsovsEphedripites sp., Murmanskaya-26, 2212.8 Early–Middle Triassic (Induan–Ladinian) palynomorph taxa from the Fersmanovskaya-1, Kurentsovskaya-1 and Murmanskaya-26 wells. Scale bar = 20µm. A. Dictyophyllidites mertonii, KurentsovsEphedripites sp., Murmanskay48.3 Early–Middle Triassic (Induan–Ladinian) palynomorph taxa from the Fersmanovskaya-1, Kurentsovskaya-1 and Murmanskaya-26 wells. Scale bar = 20µm. A. Dictyophyllidites mertonii, KurentsovsEphedripites sp., Murmanskay48.3, 2212.8uncus, Murmanskaya-26, 2347.8 Early–Middle Triassic (Induan–Ladinian) palynomorph taxa from the Fersmanovskaya-1, Kurentsovskaya-1 and Murmanskaya-26 wells. Scale bar = 20µm. A. Dictyophyllidites mertonii, KurentsovsEphedripites sp., Murmananskaya-26, 2501.9 Early–Middle Triassic (Induan–Ladinian) palynomorph taxa from the Fersmanovskaya-1, Kurentsovskaya-1 and Murmanskaya-26 wells. Scale bar = 20µm. A. Dictyophyllidites mertonii, KurentsovsEphedripites sp., Murmananskaya-26, 2501.9cus, Murrdaitina gunyalensis, Murmanskaya-26, 2501.9 E

possible to trace stratigraphic packages across from the data-rich and well-studied Norwegian parts into the more sparsely explored Russian Barents Sea. Based on all available data, reflectors corresponding to main stratigraphic boundaries were traced across the entire GBSB basin. We did not have access to seismic data in the northernmost part of the formerly disputed zone (north of 75°N), which leaves an around 175,000 km² gap between interpretations in Norwegian and Russian parts (Figure 1a). However, the correspondence between the reflectors on both sides shows that the interpretations are reasonable on both sides (Figure 4b).

Furthermore, the interpretations of stratigraphic units in seismic data have been calibrated through integration with new palynostratigraphic data (presented herein) and published datasets from Russian Barents Sea wells (Fefilova, 2001, 2005; Fefilova, 2011; Fefilova, 2013a, 2013b). These data are correlated with the recently revised palynozonal framework for the Western Barents Sea (Paterson & Mangerud, 2020; Vigran et al., 2014).

3.3 | Seismic well tie

Surfaces are defined based on well-ties of stratigraphic markers provided by the NPD based on the well operator's reports, which in turn, rely on biostratigraphy and lithostratigraphic interpretation of wireline logs (Figure 9). Stratigraphic intervals are calibrated by palynostratigraphy, which is independently calibrated by marine macrofossil occurrences from Svalbard and the Western Barents Sea (Paterson & Mangerud, 2017, data presented herein). Stratigraphic markers have been converted from depth to time by using available checkshot data from wells where these are available (Figure 9).

The imaged seismic reflectors and associated formation boundaries correspond to lithological boundaries between the deltaic topsets and overlying offshore mudstones in the majority of the basin (Figure 9). In proximal and distal parts of the basin, correlative conformities (reflectors related to varying sandstone-content in alluvial deposits, or varying

properties in offshore shales) are recognised in many areas for the flooding surfaces corresponding to the largest transgressions (Figure 10).

3.4 | Palynology

3.4.1 | Sampling, processing and analyses

Thirty-eight samples were collected from core material that span the Lower–Upper Triassic succession from seven Eastern Barents Sea wells (Figures 11 and 12). Palynology samples were processed by Palynological Laboratory Services (PLS) Ltd. using standard hydrochloric acid (HCl) and hydrofluoric acid (HF) maceration techniques, followed by oxidation in nitric acid (HNO₃) (see Traverse, 2007, p. 632–647). Analyses were conducted at the Department of Earth Science, University of Bergen, Norway and at the Geological Faculty, Moscow State University, Russia. Semi-quantitative palynomorph abundance was determined by counting 300 palynomorph specimens per sample preparation (recovery and preservation permitting). Rarer taxa were recorded as present outside of the count.

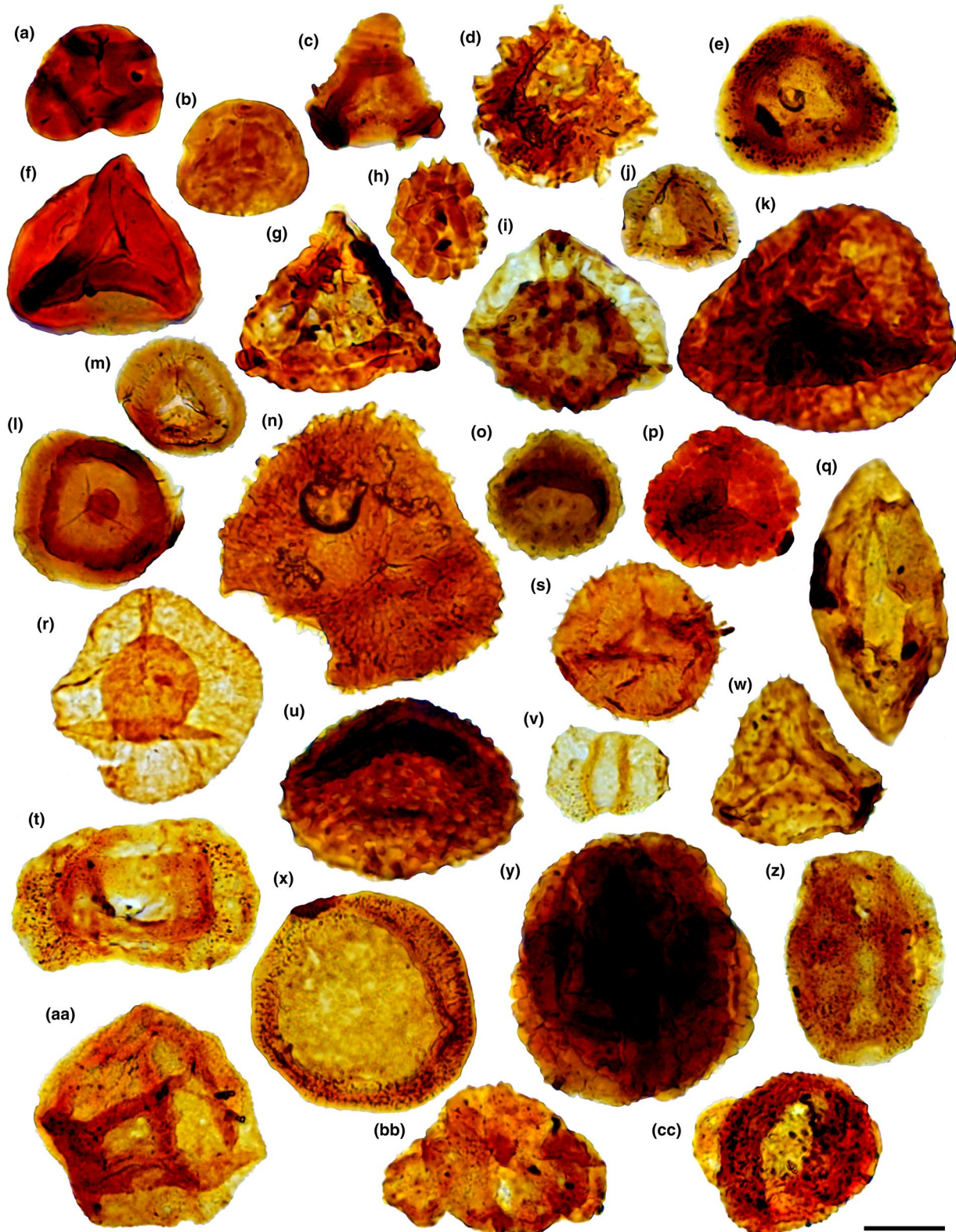
4 | RESULTS

This section describes the stratigraphic boundaries, how they were dated and traced, the thickness trends, the seismic characteristic of each of the Triassic stratigraphic units, how intrusions affected thickness differences and facies variations within stratigraphic units in different parts of the basin. Results presented herein show that more than 90% of the Triassic sediments in the GBSB were deposited by one sedimentary system derived from sources in the east that supplied more than 10¹⁸ tons of sediments. This is demonstrated by: (a) the fact that the sediment transport directions (clinofolds, channels) are correlative across the basin (b) the fact that major stratigraphic surfaces are the same across the basin, and (c) that similar and related lithologies are present over the entire basin.

4.1 | Dating of the Eastern Barents Sea wells

Core samples from the selected Eastern Barents wells were analysed for palynology to provide age constraints for the stratigraphic surfaces. A detailed description of the palynostratigraphy is presented in Supplement 1. Most samples

yielded moderately well-preserved and diverse palynological assemblages, which were comprised almost exclusively of plant spores and pollen grains (Figures 11 and 12). The scarcity of marine palynomorphs in these wells contrasts with their common occurrence in Triassic assemblages from the Western Barents Sea. Such differences likely reflect the more



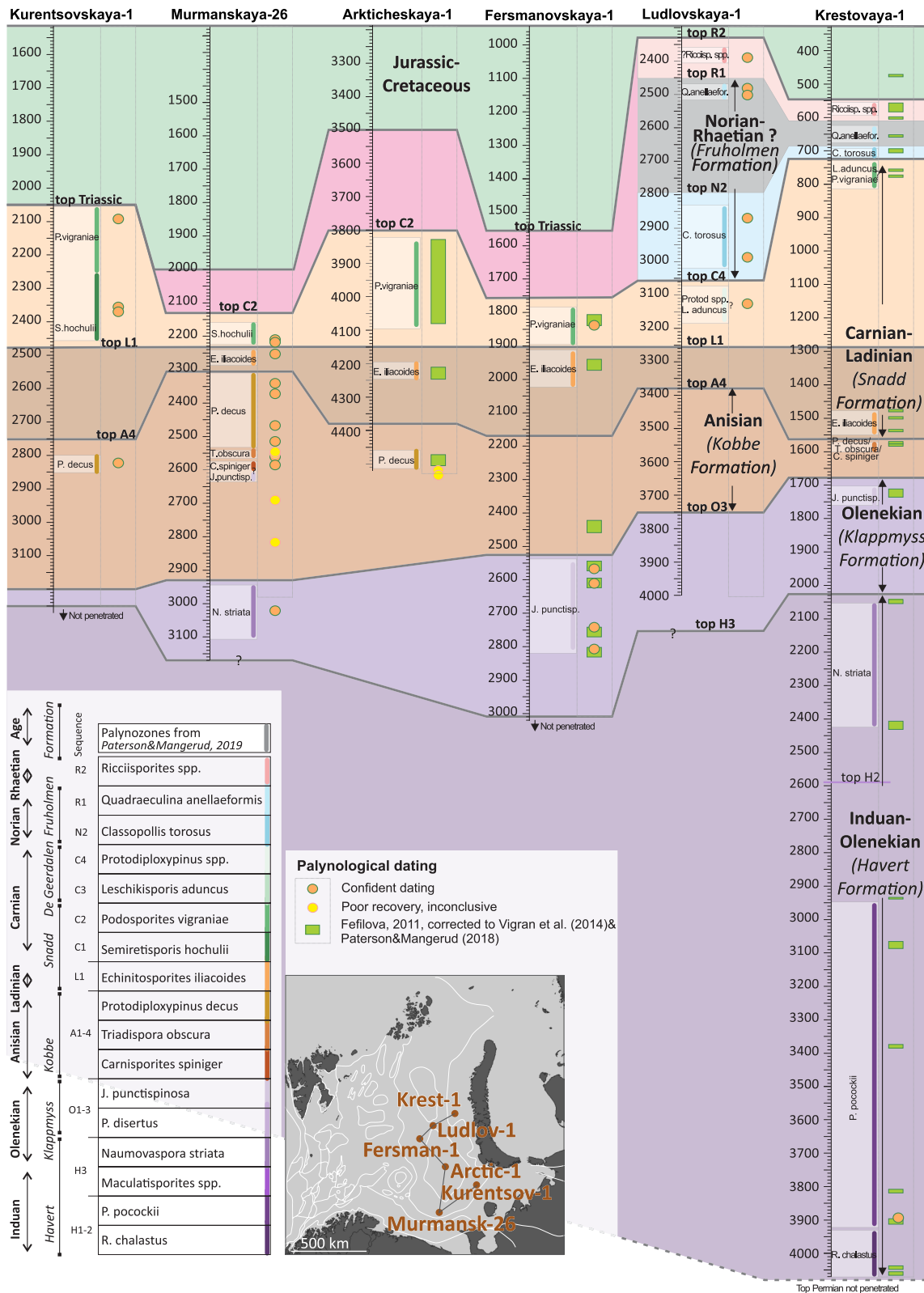


FIGURE 13 The Eastern Barents Sea well correlation panel with palynozones recognized from core samples and Fefilova (2013a, 2013b), Viskunova et al. (2000), Gavrilov et al. (2010) shows the similarity to the terrestrial floras from Western Barents Sea and Svalbard (Paterson & Mangerud, 2020). Combination palynozones with seismic interpretation (see Figure 9) shows that stratigraphic units are correlative across the GBSB

Basin: Mark et al. (2019)). For studies modelling basin subsidence (e.g. Gac et al., 2014), this effect has hitherto not been taken into account (cf. Gardiner et al., 2019) in the GBSB. Accounting for the intrusions leads to an ca. 0.5 km decrease of Triassic subsidence, and ca. 0.5 increase in Late Cretaceous subsidence.

In the eastern Barents Sea, igneous intrusions were separated into three groups (Figure 8 *cont.*): 1) sills in the lower part of Triassic succession that occur mainly between top Permian and top Induan where they are actively controlled by lithology and follow main clinoforms and major flooding surfaces; 2) sills in the upper part, between top Induan and top Triassic where they are less controlled by host rock-lithology and are mainly saucer-shaped (cf. Schofield et al. (2012); Eide et al. (2017)); and 3) as dykes (i.e. subvertical dykes) mainly imaged in the Triassic succession, controlled by tectonic structure. The dykes are mainly observed on uplifted basement highs and continue the trend that could be seen in outcrops (Dymov et al., 2011), and a magnetic map close to Franz-Josef Land (Minakov et al., 2018) and are a part of the HALIP giant radiating dyke swarm (Buchan & Ernst, 2018).

4.5 | Main stratigraphic units

4.5.1 | Induan unit—Havert Formation

In the GBSB, sedimentary wedges of the Havert Formation prograded into the basin from the east. Only minor amounts of sand-rich sediment were supplied from the other basin margins in the south and west (e.g. Eide et al., 2018). The base of this unit has variable expression in different areas of the basin and approximately coincides with the Permian–Triassic boundary. The top Induan reflection occurs as a distinctive high amplitude hard-kick (increased impedance, Figure 9) across the basin except where it is intruded in the Eastern Barents Sea. The formation is dated as latest Changhsingian–early Olenekian (249.8–251.902 Ma) by a combination of palynological (Rossi et al., 2019; Vigran et al., 2014), ammonoid (Vigran et al., 1998) and C-isotope data (Hermann et al., 2010) in the W Barents Sea, and this age is demonstrated to also be valid in the Eastern Barents sea by the palynostratigraphic data presented above.

The Induan deposits can be divided into three sub-units. The lowest sub-unit, H1, only occurs along Northern Fennoscandia, from which it prograded (Eide et al., 2018). The two other sub-units H2 and H3, prograde from the east, and downlap the lower H1 (Glørstad-Clark et al., 2010; Rossi et al., 2019). The Induan deposits prograded across the Bjarmeland Platform, and pinch out on the Loppa High, the Gardarbanken High and the southeastern part of Kong Karl Platform (Figure 10). In the St Anna Basin, northeastern part

of the GBSB, the top and bottom of units H2 and H3 contain erosional features interpreted as paleovalleys (Figure 7) which could have been associated with sediment entry points to the basin.

The Havert Formation is more than 2 km thick on Admiralty High and Eastern Barents Sea Basin and thins towards basin margins. Critically, the Induan unit does not show any thinning towards Novaya Zemlya, indicating that Novaya Zemlya was not uplifted at this time, but rather was the site of a deep, actively subsiding sedimentary basin. Greatly increased thickness occurs in the salt basins across the GBSB, such as the Nordkapp and Tiddlybanken basins (Rojo et al., 2019). This is likely because the rapid influx of large amounts of sediment led to loading and salt movement across the region. It is worth pointing out that similar thickness anomalies are observed in the Korotai Kha Basin and the Varandey-Adzvin'skaya structural zone in the Timan-Pechora Basin due to movement of the Dolginsky salt dome (Figure 5c). Deformation observed in these areas was previously interpreted to be the result of tectonic thrusting (Henriksen, Bjørnseth, et al., 2011 (Figure 10.36 i), Ivanova et al., 2011).

The Induan deposits consist mainly of clinoformal siltstones and mudstone-rich topsets with sparse, sandy fluvial channel deposits up to 3.5 km wide and 12 m thick in the western Barents Sea. In the most proximal parts of the GBSB, the Timan-Pechora Basin, the time-equivalent deposits consist of conglomeratic sandstone with volcanic material of the Charkabozh'skaya Formation.

4.5.2 | Olenekian unit—Klappmyss Formation

The overlying Klappmyss Formation is assigned to the late Olenekian (Spathian) (249.8–247.2 Ma) by palynology (Rossi et al., 2019; Vigran et al., 2014) and ammonoid faunas (Vigran et al., 1998). Seismic data indicate that the unit prograded in a northwest direction (Klausen et al., 2015; Riis et al., 2008). The top of the formation is defined by a hard kick (negative high amplitude, Figure 10) that can be traced on the Fedynsky High and across major parts of the Western Barents Sea. In the deepest part of the basin, the interpretations are somewhat unclear because of the large number of Cretaceous intrusions. Nonetheless, considering the relatively simple structure of the formation in areas without intrusions, it is generally straightforward to approximate the top and base of the unit.

The Olenekian package is characterised by three third-order clinoform packages which downlap onto the underlying Induan unit (Klausen et al., 2015). Seismic lines and thickness maps (Figure 8) of the Olenekian unit shows that an extensive topset accumulated landward of the clinoforms.

The thickness of the Olenekian unit is c 800 m in the deepest part of the Eastern Barents Sea and thins towards

the basin margins (Figure 8b). The Olenekian deposits are penetrated by 41 wells in the Southwestern Barents Sea and five wells in the Eastern Barents Sea including wells located in Franz-Josef Land, where it mainly consists of dark shales with thin sandstone beds (Dypvik et al., 1998). Our data shows that the Klappmyss Formation of the Southwestern Barents Sea is a continuation of the Kharaleyskaya Formation (Morakhovskaja, 2000) that occurs throughout the entire Timan-Pechora Basin (Figure 3), except the Korotaikha Basin in the foreland of the Ural Mountains, where it is represented by the upper part of the Lestanshorskaya Formation.

4.5.3 | Anisian unit—Kobbe Formation

The Anisian sedimentary deposits (247.2–242 Ma), corresponding to the Kobbe Formation, prograded northwestwards in the Southwestern Barents Sea, in the same manner as the other pre-Carnian packages. Regionally, the unit is bounded on the top by the marine flooding surface that corresponds to top Anisian (Figure 4) and represented as a hard-kick (high amplitude negative reflector, Figure 9). The Anisian clinoformal unit downlaps the Loppa High (Glørstad-Clark et al., 2010), Gardarbanken High, Storbanken High and Victoria High.

The Anisian package consists of four third-order clinoforms packages that are best developed in the Southwestern Barents Sea (Klausen et al., 2018). The thickness of the Anisian package is generally ca. 170 m in the topset deposits on top of the previous clinoform packages, and shows a thickening to 600 m northwest of the previous clinoform break (Figures 5 and 8c). The succession is thicker in the salt basins, up to 1,136 m thick, indicating salt movement during deposition. The fluvial channel belts are observed to be up to 5 km wide and 19 m thick in the Southwestern Barents Sea (Klausen et al., 2018).

This unit is termed the Kobbe Formation in the Southwestern Barents Sea and is the time equivalent to the lower part of the Anguranskaya Formation in the Timan-Pechora Basin where the thickness is up to 240 m (Morakhovskaja, 2000). No evidence of marine incursions is reported in the Timan-Pechora Basin during this time.

4.5.4 | Ladinian unit—Snadd Formation

The least voluminous, Easterly-derived, second-order sequence in the GBSB is the Ladinian sedimentary wedge (242–237 Ma). The deposits are assigned to the lowermost Snadd Formation (Figure 3). Palynological and ammonoid data (Paterson & Mangerud, 2017, 2020; Vigran et al., 1998, 2014) indicates a Ladinian age. This is consistent with

rhenuium–osmium (Re–Os) dating of shallow stratigraphical cores from offshore Kong Karls Land (Xu et al., 2014).

Following the trend of progradation for the previous Triassic units, the Ladinian clinoform package is observed northwest of the Bjarmeland Platform. In more proximal areas, it mainly occurs as a tabular set of reflectors (Figure 4), because the water depth was not sufficiently deep for seismically imageable clinoforms to form (cf. Klausen et al., 2018). The Ladinian package is the first to prograde out of the GBSB and into the deeply buried basins on the Atlantic margin of the Barents Sea (Figures 8d,f and 4a). Because of poor seismic quality, deep burial and complicated tectonic deformation, the sedimentary packages have not been interpreted westward of the GBSB.

It is difficult to distinguish the Ladinian to Norian sedimentary units in the Eastern Barents Sea because the post-Anisian deposits here all occur as parallel reflectors without any candidates for major flooding surfaces (see Figure 3), thus palynological data is particularly useful. In the northwest GBSB, the Ladinian unit is clearly defined between well-developed flooding surfaces.

Considering that the Ladinian succession is developed as a tabular topset and a thick package of clinoforms in front of the previous shelf break (Figure 8 *cont.*), the increased thickness observed in the Franz-Josef Land wells probably shows that there are similar clinoform packages present there as well. This agrees with the thickness maps of this unit, which show a linear belt of high thicknesses extending to Franz Josef Land (Figure 8 *cont.*).

4.5.5 | Carnian-Norian unit—Snadd Formation

The Carnian succession (237–227 Ma) can be divided into five sub-units in the distal parts of the system (western GBSB). These units are difficult to trace into the proximal Eastern Barents Sea because the marine shales associated with flooding surfaces become too thin to confidently interpret in seismic data and finally pinch out. This interval contains exceptionally well-imaged amplitude anomalies (units C1-3) that clearly correspond to fluvial channel belts in 3D seismic and core (Klausen et al., 2014, Figure 4a). In the Timan-Pechora Basin, the most proximal part of the study area, the Carnian succession is entirely terrestrial, but there is a variation of terrestrial and marine deposits in Southwestern and Northwestern Barents Sea. Similarly, no marine sediments occur in this time interval during the middle-late Carnian (C3 and C4) succession in the Eastern Barents Sea and Timan-Pechora basins. In these proximal locations, the Carnian-Norian succession comprises a stacked series of fluvial channels complexes, each up to 50 m thick. On Svalbard, the deposits of the Tschermakfjellet Formation

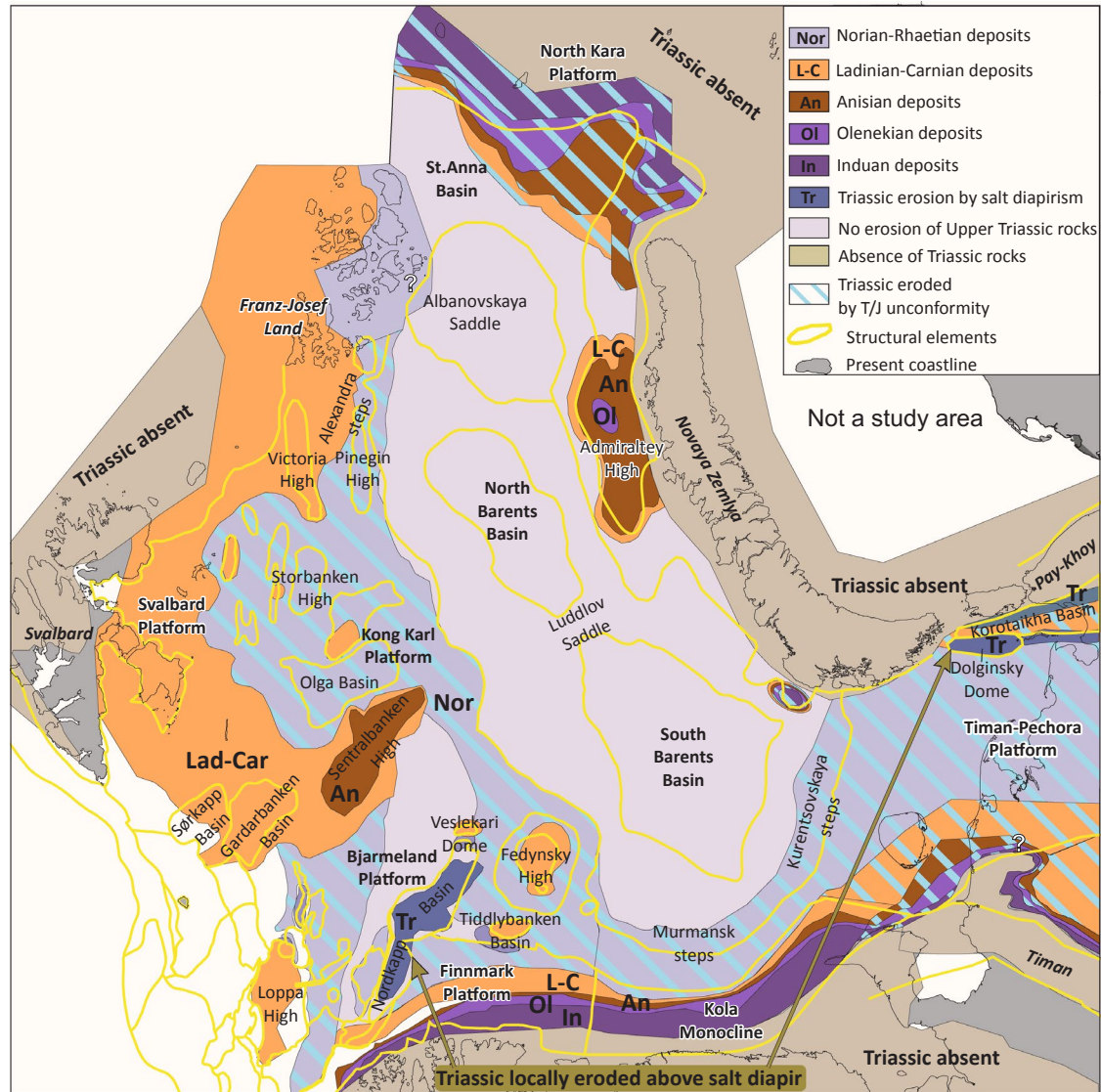


FIGURE 14 Truncation trends in the Greater Barents Sea Basin. An observation based on structural maps, outcrop geological map and Müller et al. (2019). Colours correspond with the Triassic units, a light purple shows area with no erosion of the Upper Triassic rocks. Colours without blue stripes show area where the Triassic was eroded during the Cenozoic; blue stripes marked the area where the Triassic was eroded by the Triassic/Jurassic unconformity (Rhaetian unconformity)

are the onshore equivalents of the Snadd Formations and represent the distal part of the same prograding sedimentary system sourced from the east (Figure 3).

Carnian C1

The top boundary of the Carnian C1 unit is the intra Carnian flooding surface (Klausen et al., 2015). Palynological evidence indicates that the C1 unit was deposited in the early Carnian (early Julian, ca. 237–235.9 Ma) (Paterson & Mangerud, 2017). The thickness map of the interval (Figure 8, *cont.*) shows the southwest-northeast trend across the Greater Barents Sea Basin; the lower Carnian C1 wedge is more extensive and contains internal clinoforms of smaller order than what has been recorded in the

following units. Areas on the Atlantic Margin, west of the GBSB, are buried below ca. 3 km thick packages of the Cretaceous and Paleogene deposits, and are strongly faulted making seismic interpretations difficult. Wells 7220/8-1, 7219/12-1 and 7321/8-1 have penetrated up to 600-m thick deposits of Carnian age in this area. These observations document that large amounts of lower Carnian deposits prograded west and northwest of the present-day Barents Sea Basin, but due to the depth of burial and relatively poor seismic resolution, it is difficult to define the volume of Carnian sediments here with certainty. Clinoformal packages are observed on the Bjarmeland, Kong Karls Land and Svalbard platforms (Figures 4–7). The topset of these clinoforms can be traced into more proximal areas in Finnmark

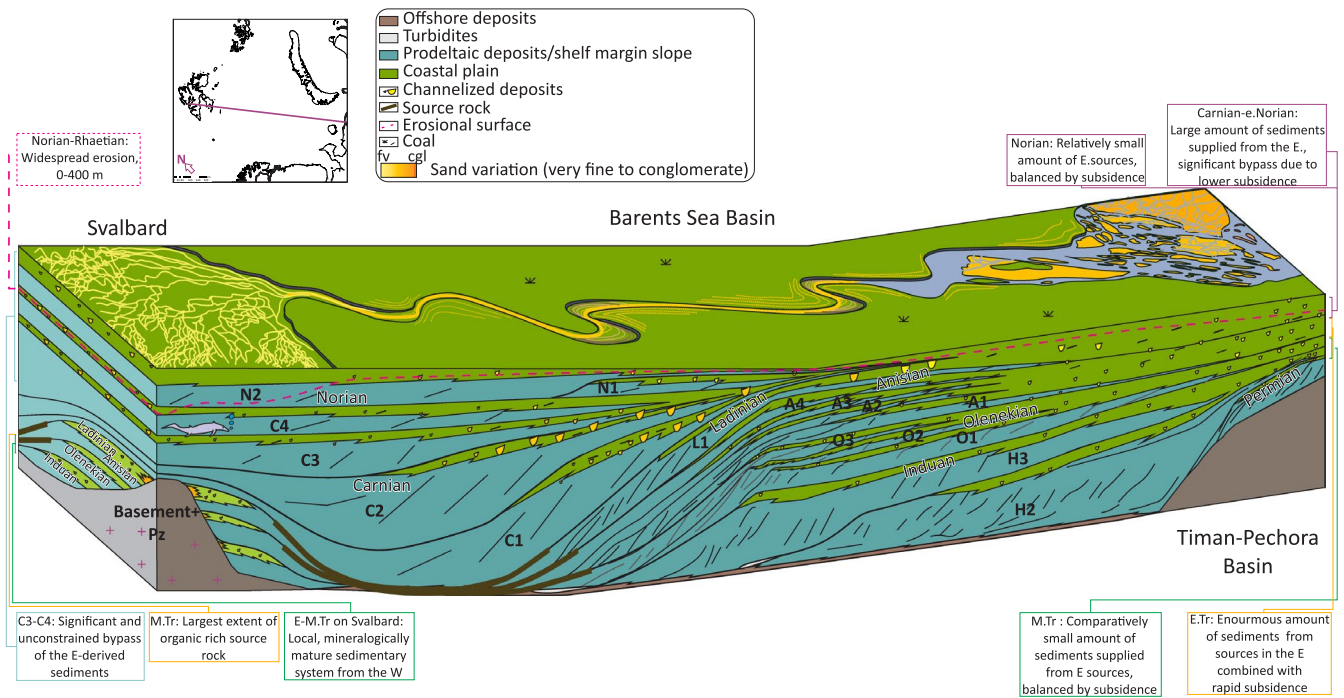


FIGURE 15 Conceptual sedimentological model of Triassic succession from Timan-Pechora to Svalbard, not to scale, with northwestward progradational infill, backstepping some of the units (e.g. Olenekian and N1) and thickness changes in the profile. Erosional surface ideal picture by Rhaetian time

Platform, the eastern part of the Bjarmeland, Kong Karls Land, Svalbard platforms and the whole eastern Barents Sea (Klausen et al., 2014, 2016).

Carnian C2

The C2 unit is observed in seismic data in the western part of the basin; the top boundary is a high amplitude hard kick and easily traceable in platform parts (from Fedynsky High in the east until Western Margin and from Pinegin High to Svalbard) (Figures 5–7). Palynological evidence indicates that it was deposited during the late Julian (c. 235.9–234.8 Ma) (Paterson & Mangerud, 2017). In the same way, as the previous Ladinian L1 and C1 units, the Eastern Barents Sea comprises proximal part of the Upper Triassic succession (Figure 9). The thickness of this unit in the Southwestern Barents Sea is up to 250 m (Figure 8 *contn.*).

Carnian C3, C4 and Norian N1 (De Geerdalen Formation on Svalbard)

The C3 sub-unit is similar to C1 in that it also contains high amplitude reflectors interpreted as channels (Figure 15), which are easily identified in 3D seismic. The unit thins towards the east and starts to be mappable from the western Nordkapp Basin. It is locally present in the Southwestern Barents Sea where it contains smaller order clinofolds. On Hopen and offshore Kong Karls Land, the C3 unit is dated as approximately late Julian

to Tuvallian 2–3 by palynology (Paterson & Mangerud, 2015; Paterson et al., 2017), calibrated by Re-Os dating (Xu et al., 2014), and ammonoid faunas (Korchinskaya & Semevskij, 1980; Smith, 1982) from the over- and underlying units respectively.

Clinofolds of the overlying C4 unit are not discernible in the southern Barents Sea (Figure 15). It only occurs as topset deposits which cannot be separated from the underlying C3 unit. In the Northwestern Barents Sea, however, it is clearly mappable. It prograded northwards towards Hopen, Edgeøya and eastern and central Spitsbergen where both C3 and C4 are exposed in outcrop, and reaches a thickness of 435 m (e.g. Vigran et al., 2014). Paterson and Mangerud (2015), Paterson and Mangerud (2017) have assigned a late Tuvallian age for this unit based on palynological evidence, independently constrained by magnetostratigraphy (Lord et al., 2014) and ammonoid occurrences on Hopen (Korchinskaya & Semevskij, 1980; Smith, 1982). This C3 unit is present as a relatively thick package at the most western and northern parts of the basin, and this indicates that great amounts of sediments must have also been deposited northwestwards of the studied GBSB.

The uppermost unit of this package, the early Norian N1 unit has a high amplitude top reflector which is easy traceable east of the Loppa High in Southwestern Barents Sea but is difficult to discern due to strong faulting in the western part. The unit contains third-order small scale clinofolds

that have their shelf-break at least 300 km southeast from the minimum position of the C4 package, and therefore represents a backstepping of the system (see Figure 3). The N1 sequence is principally dated by palynological evidence (e.g. Paterson & Mangerud, 2020) calibrated by occurrences of early Norian (Lacian) ammonoids in the Flatsalen Formation on Hopen (Korchinskaya & Semevskij, 1980; Smith, 1982).

4.5.6 | Norian–Rhaetian unit

N2-R1—Fruholmen Formation

The upper part of the Upper Triassic, corresponding to the Fruholmen Formation in the W Barents Sea, is completely or partly eroded in most parts of the GBSB (apart from the deeper basins in the Eastern Barents Sea, the Atlantic margin and in salt basins), by either the base Quaternary erosion (Upper regional unconformity, URU) or by erosion at the Triassic/Jurassic Unconformity (Figure 14) (Müller et al., 2019). Rhaetian deposits have also been recorded onshore, on Hopen and Kong Karls Land (Paterson and Mangerud, 2015; Smelror et al., 2019), and offshore in the Hammerfest and Nordkapp basins (Paterson & Mangerud, 2017, 2019; Vigran et al., 2014). The unit is also relatively thin in most of the study area (ca. 50 m on the Bjarmeland Platform, versus 579 m on the Atlantic margin and in the Eastern Barents Sea), making it difficult to trace on regional seismic data. It is therefore not investigated in the same level of detail as the other stratigraphic units.

Similar to the preceding Triassic units, the N2-R1 deposits contain a lower marine mudstone and an upper progradational deltaic topset with channels (Figure 15). This unit is generally thinner and has been deposited over a longer time span than the previous units. However, the thickness is poorly constrained due to extensive erosion by the Rhaetian unconformity (Müller et al., 2019; Figures 14 and 3). Because the depositional thickness of the Norian–Rhaetian succession is so poorly constrained by seismic data, defining the thickness of it across the GBSB, is beyond the scope of this study.

4.6 | Large-scale thickness trends

The Triassic succession prograded in a northwesterly direction towards the Svalbard Archipelago (Klausen et al., 2014; Lundschieen et al., 2014) and is characterised by two different thickness trends: (1) thick deposits in the SE parts and (2) thin deposits in the northwestern parts of the basin for the Early Triassic, a trend that reverses in the Late Triassic (Glørstad-Clark et al., 2010). The results presented here show that the following depositional trends dominated throughout

the entire GBSB (also in the Eastern Barents Sea) during the Triassic Period.

The Induan deposits are thickest in South and North Barents depressions in the Eastern Barents Sea. The thickness map (Figure 8a) of the unit shows the general thinning towards the west and northwest (Figure 4). The unit becomes thinner towards Timan-Pechora Basin, as well as east of the St. Anna Basin where it is eroded towards the east close to Novaya Zemlya by the Triassic-Jurassic unconformity (cf. Figure 3). The Induan deposits are eroded by the Upper Regional Unconformity (URU) of Pleistocene age along the basin margins along Northern Fennoscandia and the Kara Sea (Figure 14). The Olenekian unit follows mainly the same pattern as the Induan, but it is much thinner and does not show the pronounced thickening into the Eastern Barents Sea Basin (Figure 8b). In the westernmost part of the basin, the maximum progradational extent of the Olenekian is ca. 35 km shorter than the underlying Induan package (Figure 4).

The thickness map of the Anisian unit is similar to the Olenekian and thins towards the west and northwest (Figure 8). The thickness increases in the Pay-Khoy foreland, but on the rest of Timan-Pechora Basin territory, the sedimentary package shows a constant thickness. The Anisian unit progrades ca. 55 km further than the previous Olenekian unit (Figure 10), filling the accommodation space formed in front of it. Maximum thicknesses are shifted westward towards the Bjarmeland Platform, Loppa High, Hammerfest Basin and Kong Karls Land (Figure 8).

The thickness of the Ladinian, Carnian and early Norian deposits are shown together in Figure 8 because the flooding surfaces between the internal subunits cannot be traced further east than the Norway–Russia border. This sedimentary package shows a different thickness trend from the previous units and is characterised by minimum thickness in the east and a maximum thickness to the west. Typical thicknesses are 0.8 km in the eastern parts of the GBSB and 1.9 km in the western GBSB. The western depocentre is elongated from the Hammerfest Basin in the south to Franz-Josef Land in the north. This elongation is mainly because the deposits filled the accommodation in front of the previous clinoform succession (Figure 5).

In the western Barents Sea, the Ladinian, Carnian and Norian deposits can be divided into six subunits, defined in Klausen et al. (2015): L1, C1-4 and N1-2. The thickness map of the Ladinian unit (L1) shows a clear trend where the thickest part forms an elongate trend from the southwest in the Hammerfest Basin to northeast to Franz-Josef Land. The thickest part of the Ladinian unit is related to accommodation available in front of the Anisian package and thins towards the west and northwest as the unit pinches out. The topset thins towards the east and becomes indistinguishable from the topset of the Carnian unit just east of the Norway–Russia border.

In the Eastern Barents Sea, the Carnian package is relatively thin (ca. 300 m in the Arcticheskaya-1 well) and increases in

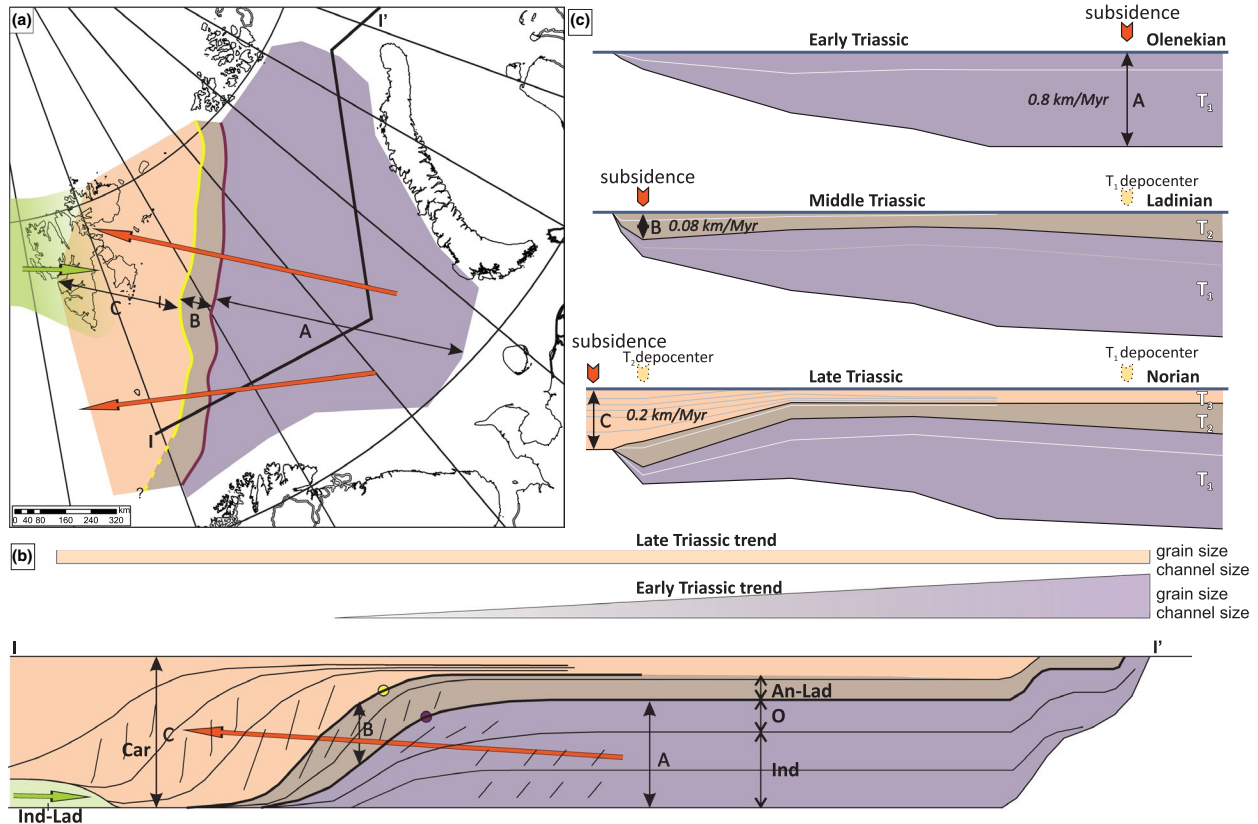


FIGURE 16 Schematic distribution of thicknesses (corrected for intrusion thickness) and main depocentre shift. The map shows the primary progradational trend (orange) and location of depocentres from southeast to the northwest and the local western source (green) on Svalbard that was mainly active during the Early and Middle Triassic. The Early Triassic trend indicates the decrease of grain size and possibly a channel size as well from proximal to the distal part of the basin; the Late Triassic trend indicates that the average grain size relatively equal across the basin and channel size varies from 25 to 50 m across the basin

thickness towards the Western Barents Sea to 1,395 m in well 7321/8-1. In the western part of the Barents Sea, the Carnian units C1-2 show a progressive progradation towards Svalbard (Figures 8, 10). In Svalbard, deposition of relatively mature sands derived from Greenland and local basinal highs ended with the arrival of the easterly depositional system of the C3 and C4 units in the Carnian (e.g. Bue & Andresen, 2014; Klausen et al., 2015). The transgressive Norian unit N1 is very thin and eroded in the west and northwest (Klausen et al., 2015; Lord et al., 2019). The unit N2, which makes up the Fruholmen Formation, is thin and partly eroded across the GBSB, and shows thickening towards the western margin but is eroded on Svalbard Figure 3 (Klausen et al., 2019).

5 | DISCUSSION

5.1 | Main uncertainties and limitations to tracing large-scale flooding surfaces

In this project, we have investigated a vast area ($1,200 \times 1,800$ km, $2,500,000$ km², Figure 1a). In some

locations, we have good control of the age and architecture of deposits because of an abundance of wells, 3D seismic data (Southwestern Barents Sea) or outcrops (Svalbard).

The greatest uncertainty is in the Eastern Barents Sea where large amounts of the Cretaceous igneous intrusions are present (Figures 4–7). The great depth of the basin (up to 10 km to the base of the Triassic) also causes uncertainties in the mapping of stratigraphic units since no wells are penetrating Induan and Olenekian at these great depths. The northern part of the East Barents Sea and the North Kara Sea have no wells at all, with the nearest wells located in Franz Josef Land (Dypvik et al., 1998) (Figure 1).

The stratigraphic framework in this study (Figure 3) is based on a set of continuous and regionally traceable marine flooding surfaces (Figures 4 and 9). Despite the uncertainties listed above, the Lower Triassic deposits are tabular in all parts of the basin, have excellent biostratigraphic age control, and the flooding surfaces are easy to identify on seismic data. In the Early Triassic, many of these surfaces are traceable all the way into the easternmost parts of the GBSB. The large extent of these surfaces is likely due to the fact that the coastal plain had a very low gradient, as should be expected

in subsiding sedimentary basins (Nyberg & Howell, 2015), and that marine transgressions could therefore penetrate far onto the coastal plain. The coastline prograded further basinward in the Middle and Late Triassic, which prevented marine transgressions from reaching the Eastern part of the GBSB. This explains why the marine flooding surfaces, and marine palynomorphs, are not found in Timan-Pechora Basin after Middle and Late Triassic. In addition to the flooding surfaces, the thicknesses and age of units fits excellently with the stratigraphy in the Timan-Pechora Basin (Figures 2 and 3). There is, therefore, a good reason to believe the seismic interpretations in areas without well control are correct.

5.2 | Large-scale depocentre change and trends across the basin

From both the seismic cross-sections and the thickness maps presented above (Figures 4–8), a three-stage shift in depocentre in the GBSB is evident (Figure 16): (A) a *Lower Triassic* thick depocentre located in Eastern Barents Sea; (B) a *Middle Triassic* transitional deposits with thin deposits located above and slightly in front of the Lower Triassic package and (C) *Upper Triassic* thick depocentre located in Western Barents Sea. Each stage is discussed in detail below.

5.2.1 | Lower Triassic southeastern depocentre

During the Early Triassic (Induan and Olenekian), the delta system prograded westwards from the east as far as the middle of the present-day Barents Sea (Figure 8). The depocentre of Induan and Olenekian packages is located in the Eastern part of the basin (South Barents Sea depression, Ludlow Saddle) and these packages thin towards the west and northwest. A marked decrease in channel size and grain size occurs within this package from proximal to distal: In the proximal Timan-Pechora Basin, the maximum observed channel belt thickness is ca. 62 m (Morakhovskaja, 2000); in the more medial Eastern Barents Sea Basin, maximum described channel belt thicknesses are 50 m (in the Krestovaya-1 well, (Norina et al., 2014)). In the Western Barents Sea, for example, in the 7226/2-1 well, the maximum described channel belt thickness is as low as 12 m (Eide et al., 2018). Similar trends in channel complex width are difficult to ascertain across the basin due to the lack of available 3D seismic data in the Eastern part of the study area. Grain size shows a similar decrease towards the northeast, with conglomerate being common in fluvial channel deposits in the Timan-Pechora Basin, whereas any grains coarser than fine sand are only very sparsely observed in

wells in the southwest Barents Sea. This clearly indicates a proximal–distal trend, and that the sediment source in this time interval must have been very close to the Timan-Pechora Basin. The Lower Triassic sediment package is considerably thicker than the overlying units, (ca. 3.5 km, vs. 0.9 and 2.0 km for the Middle and Upper (Carnian) Triassic packages), despite being deposited over a shorter interval (5.1 Myr vs. 10.1 and 8.6 Myr respectively).

5.2.2 | Middle Triassic transitional depocentre

During the Middle Triassic (Anisian and Ladinian), the main depocentre shifted slightly towards the north-northwest, and the sedimentary package prograded further across Bjarmeland Platform, Loppa High, Sentralbanken High and Kong Karl Platform (Figures 4–8). Middle Triassic clinoform packages are relatively thin in the eastern part and also thinning towards the northwest where they pinch out. Channel belt thicknesses in the Timan-Pechora Basin vary from 40 to 50 m, which is thicker than what is observed in the Southwestern Barents Sea, where it is only up to 19 m thick (Kobbe Formation, (Klausen et al., 2018)).

5.2.3 | Late Triassic northwestern depocentre

In the Late Triassic, progradation rates noticeably increased and the delta front reached at least as far northwest as Svalbard (Figures 10 and 15). How much farther the delta reached is difficult to determine because no exposure exists northwest of central Svalbard. During the Carnian, all structural elements westwards and northwestwards of Bjarmeland Platform, Loppa High, Sentralbanken High and Kong Karl Platform subsided and were buried by tabular deposits sourced from the main sediment source in the southeast. The Carnian package is relatively thin (c. 300 m) in the Eastern Barents Sea but up to 1,400 towards the northwest. Channel thickness throughout Upper Triassic varies from 30 to 50 m. Average grain size is relatively equal across the basin; the content of conglomerate in Upper Triassic deposits is low in the most proximal parts of the GBSB. This implies that the system is much longer than in the Early Triassic, and that the gradients in the source-area close to the most proximal parts of the basin must have been much lower in the Late Triassic than during the Early Triassic.

5.2.4 | Reasons for depocentre shift

This depocentre shift is likely related to two factors: subsidence and sediment supply. Huge amounts of sediment were

supplied from the eastern source in the Early Triassic, and the southeastern parts of the basin subsided rapidly to accommodate these sediments (Figure 16). Much smaller quantities of sediment were supplied during the Middle Triassic, and little subsidence was needed to accommodate these sediments. The Late Triassic package is associated with a renewed increase in sediment supply, but no simultaneous increase in subsidence rates in the southeastern parts of the basin. Very little subsidence occurred in the eastern parts of the basin, but subsidence occurred in the northeastern parts of the basin around Svalbard (Figure 16) in similar amounts to what have been observed for the Lower Triassic. However, the rates of subsidence in the Eastern Barents Sea (3.5 km over 4.6 Myr = 0.8 km/Myr) were four times higher than the rates of subsidence around Svalbard in the Late Triassic (2 km over 9.5 Myr = 0.2 km/Myr).

It is likely that the great supply of mud-rich sediment during the Early Triassic is related to both volcanism in the Siberian Traps Large Igneous Province (c.f. Reichow et al., 2009; Wignall, 2001) and volcanic uplift of the surrounding uplands including the Taimyr. It may also be speculated that the strong subsidence around the Siberian Traps in the Early Triassic is related to the displacement of the mantle due to great magmatic activity in the Siberian Traps at this time (cf. Friedrich et al., 2018).

The decrease in subsidence and sediment supply during the Middle Triassic is likely related to relative quiescence in tectonics in the source areas during this time. It is also worth noting the potential extra accommodation created by the compaction of large amounts of mudstone (e.g. Flint et al., 2009), which would add to the accommodation space created by crustal subsidence.

During the Late Triassic, the main reason for the increased sediment supply is likely to be renewed tectonic activity associated with further contraction of the Ural orogeny and in particular the initial uplift of the Novaya Zemlya orogen (e.g. Klausen et al., 2015; Zhang et al., 2018). The climate also became more humid in the GBSB, and in northern Pangea in general, in part due to northward continental drift out of the arid subtropics and into more humid latitudes (e.g. Francis, 1994; Jarsve et al., 2014). This led to an increase in both weathering and transport capacity of rivers. A major, worldwide humid episode linked to climate change during the Carnian, the Carnian Pluvial Event (Mueller et al., 2016; Ruffell et al., 2016; Simms & Ruffell, 1989; Xu et al., 2014) might also be partly responsible for greater sediment supply in the Triassic Barents Sea. The subsidence pattern in the Late Triassic likely reflects the fact that the subsidence potential in the Eastern Barents Sea Basin was already exhausted in the Early Triassic. Therefore, sediments likely bypassed in the east, and found accommodation in the Northwestern Barents Sea.

5.3 | Tectonic evolution of the Polar Urals and Novaya Zemlya

The Polar Urals and Novaya Zemlya Fold and Thrust Belt (NZFTB) were uplifted in the Late Triassic–Early Jurassic, but the exact timing and relative magnitude of uplift remains poorly constrained partly due to lack of data. Recent apatite fission track analysis from Novaya Zemlya by Zhang et al. (2018) shows rapid cooling between 220 and 210 Ma, indicating that uplift occurred in the late Norian–Rhaetian. Müller et al. (2019) proposed that the latest Triassic *Rhaetian unconformity* across the GBSB was caused by the Late Triassic uplift of the Polar Urals and Novaya Zemlya. The present study presents the largest database and best coverage of seismic surveys and wells around the NZFTB, and although it is clear that more data are needed to constrain the timing, magnitude and spatial distribution of uplift, we have made the following observations that relate to the evolution of Novaya Zemlya in the Triassic:

1. There are ca. 3 km thick Lower–Middle Triassic deposits that can be traced all the way to the NZFTB, without any indications of thinning. This implies that the NZFTB was a basin during the Early Triassic, and that uplift must have occurred later than the Middle Triassic (Figures 4 and 8)
2. There is an angular unconformity at the base Jurassic (Figures 5c and 7) with erosion down to the Anisian (Kobbe Formation) observed both north and south of the NZFTB (Figures 14 and 4).

The base Jurassic/Rhaetian unconformity can be traced on seismic data into the Western Barents Sea, where it corresponds to basin inversion and salt dome reactivation in the Norwegian sector of the Barents Sea, which occurred approximately in the Rhaetian (Müller et al., 2019). It seems safe to assume that the age of uplift in the W Barents corresponds to the culmination of uplift in the NZFTB, and thus the uplift here must have occurred sometime between the Anisian and the Rhaetian (Figures 8 and 4). It is possible that changes in the sedimentary systems in the GBSB in the late Carnian indicate early tectonic uplift in the NZFTB. These changes include the sudden progradational nature of the Carnian C3–4 unit compared to the C1–2 unit (this study), change to more westerly sediment transport directions and change to smaller and more abundant fluvial channels in the C3–4 unit compared to the C1–2 unit (Klausen et al., 2015), the appearance of recycled quartz grains (grains with dust-rims and fluid inclusions encased in younger cement) in the Snadd Formation and appearance of young zircons in the Snadd Formation (Fleming et al., 2016). Moreover, the overspill of the Upper Triassic sediments into adjacent

basins (discussed below) also indicates strong uplift in the source area, and uplift in the NZFTB is the most likely candidate for that. Thus, the earliest tectonic evidence of uplift might be evident in the late Carnian, giving a protracted uplift of the NZFTB that culminated in the Rhaetian–Early Jurassic.

5.4 | Implications for provenance studies in the GBSB

On Svalbard, the Lower and Middle Triassic deposits show great mineralogical maturity and are sourced from the west (Greenland and local sources, Bue & Andresen, 2014; Mørk, Dallmann, et al., 1999; Mørk, Elvebakk, et al., 1999). In the Carnian, the mineralogy shows a definite change to less mature sediments, and it is evident that these lithologies are derived from the eastern source (Bue & Andresen, 2014; Mørk, Dallmann, et al., 1999; Mørk, Elvebakk, et al., 1999). However, the Taimyr Orogen has been proposed as a source for the late Carnian age De Geerdalen Formation on Svalbard (Fleming et al., 2016) based on the presence of young zircons in that interval that have not been found in the Southwestern Barents Sea. These authors suggested that the hypothesised Carnian progradation from Taimyr had not been recognised by studies based on seismic data, because of the lack of seismic data from the northern GBSB. In this study, we have now analysed seismic data from the entire northern region of the GBSB, and the northern areas show a persistent northwest progradation direction through the Triassic, including the late Carnian (Figure 10). Although we do not have access to 3D seismic data from the area, which is needed to determine channel directions, the direction of sediment transport measured from the clinoform directions make a source in Taimyr unlikely. We, therefore, suggest that more detrital zircon ages throughout the GBSB region are needed to better understand the distribution and source of these young zircons, especially from the youngest part of the Carnian deposits where these are abundant. Furthermore, the stratigraphic framework presented in this contribution (Figure 3) will make it possible to design studies in a way that geographical and temporal variations can be isolated in provenance studies.

5.5 | Sediment bypass into other Arctic basins

In the Triassic, there was a large, semi-enclosed shelf underlain by continental crust north of the GBSB, which comprised the Lomonosov Ridge, the Sverdrup Basin, the Chukchi Borderland and Alaska (Shephard et al., 2013; Sømme et al., 2018). The exact location of the different

microcontinents remains controversial (cf. Miller et al., 2018; Nikishin et al., 2019), and it is possible that the locations of these could be constrained by combining detailed provenance work in these regions with the timing of overspill presented in this study.

The western and northern margins of the GBSB were rifted off in the Palaeocene–Eocene and Late Cretaceous, respectively (e.g. Doré et al., 1999; Faleide et al., 2008; Seton et al., 2012). Our analysis of seismic data of the Triassic of the GBSB shows that there are northwest-dipping clinoforms (i.e. indicating sediment transport towards northwest) as far towards the basin margin as there is seismic data, and as far towards the west as until the Triassic is faulted and buried so deeply that it cannot be interpreted confidently, or until the basin margin itself. This strongly suggests that the Triassic sedimentary system prograded beyond the present-day GBSB, and that sediments derived from the eastern sources were deposited into adjacent basins. Furthermore, based on the sediment transport directions that can be deduced from the seismic data, we expect overspill from the easterly sedimentary system (1) throughout the Triassic N of Franz-Josef Land and the Sant Anna Basin, (2) along the Atlantic Margin S of the Loppa High from the Ladinian and (3) along the entire Northern and Western margins of the GBSB and northwest of Svalbard during the Carnian and possibly early Norian (Figures 10 and 15). The Norian–Rhaetian uplift episode described by Müller et al. (2019) likely also made it possible for sediments from the eastern source to reach basins to the north and west of the GBSB. Thus, the seismic data indicates a potential for significant overspill from the GBSB in the (1) late Carnian–earliest Norian and in the (2) late Norian–Rhaetian.

In a study from the Sverdrup Basin, Anfinson et al. (2016) interpreted an Ural source of Carnian and Norian deposits in the northern part of the Sverdrup Basin where, especially in the Norian, large amounts of sediments arrived in the basin. Based on plate reconstructions at ca. 200 Ma (Seton et al., 2012), North Ellesmere Island was located in an area where it was likely reached by the Carnian–Norian sedimentary system sourced from the eastern sources (Figure 10). A provenance shift in other Arctic basins (e.g. Chukchi basin, Wrangel Island, New Siberian Islands) was documented Miller et al. (2013), Miller et al. (2018) and Ershova et al. (2015). Their studies suggest a close proximity to the Siberian Traps and sediments sourced from West Siberia, Taimyr and Polar Urals during the Triassic and sediment transportation across the GBSB.

The Lomonosov Ridge is a microcontinent to the north of the GBSB and was rifted off in the early Eocene (Doré et al., 2016; Grantz et al., 2001; Nikishin et al., 2017; Pease et al., 2014). Samples from the Lomonosov Ridge are limited, but from the clinoform directions (Figure 10) and

thicknesses mapped (Figure 8) in this study, it appears highly likely that great thicknesses of Triassic deposits should exist in the Lomonosov Ridge, with the oldest Triassic deposits towards the southeast and Carnian-Norian deposits towards the northwest. Sediments may also have prograded onwards from the Lomonosov Ridge to basins beyond.

Thick faulted packages of the Upper Triassic are located on the Atlantic (Western) margin of the GBSB, but these are buried by thick packages of the Jurassic to Quaternary sediments and are difficult to interpret in the seismic datasets we have access to. More data are required to determine where the boundary between sediments derived from Greenland (c.f. Bjerager et al., 2019) and the sediments derived from the eastern sources were located in the Carnian.

5.6 | Implications for petroleum exploration

Understanding the distribution of different sedimentary systems within the basin makes it possible to extrapolate knowledge from well-studied areas into areas with little data (e.g. Helland-Hansen et al., 2016). The sedimentary system of the large GBSB was fed by a continental scale catchment, and the deposits are relatively well understood due to widespread hydrocarbon exploration in the Timan-Pechora Basin and the Southwestern Barents Sea, with analogues in large, continuous outcrops on Svalbard (Figure 1).

In the southernmost part of the Southwestern Barents Sea, the earliest Triassic H1 unit and also most other stratigraphic units, are relatively sand-rich due to the supply of sand from Fennoscandia (Eide et al., 2018; Fleming et al., 2016), such as in the Goliat Field (Duran et al., 2013). In the Timan-Pechora Basin, which is the most proximal part of the study area, the Peschanoozerskoe and Tarkskoe fields contain the main reservoir in Lower Triassic channelised deposits (Charkabozhskaya Formation) that despite good porosity contain up to 75% of expansive clay material as smectite and montmorillonite (Toporkov & Denisenko, 2008). Here the location of the fields closest to the source shows both coarser grain size and larger channels, but also more poorly sorted and clay-rich deposits typical of proximal terrestrial deposits. On Svalbard, the majority of sandstone is in the channel belt complexes, and although the proportion of channels is not particularly high (c.10%), in the Carnian De Geerdalen Formation, the sandstone properties are good (porosity ca. 30% in channels; Haile et al., 2018).

Despite the mudstone-dominated nature of the Triassic interval, multiple oil and gas discoveries have been made in this interval in the Southwestern Barents Sea. The discoveries have mainly been in channel belt complexes that are well-imaged in 3D seismic data. It is evident that there is potential for channelised sandstone reservoirs in the northern part of the Barents Sea, and in this distal position the source rock in the

Steinkobbe Formation is more favourably positioned directly beneath good reservoir rocks (Lundschien et al., 2014). The present study indicates the limits of terrestrial facies at different times in the Upper Triassic and shows the larger source to sink setting in which these reservoir sandstones must be considered.

Offshore marine deposits that are associated with the best quality of source rock (kerogen types I and II), developed in the western and northwestern part of the GBSB in the Botneheia and Steinkobbe Formation (Figure 3) (Abay et al., 2018; Leith et al., 1993; Vigran et al., 2008). In the more proximal areas, such as the Southwestern and Eastern Barents Sea, the Lower and Middle Triassic deposits are characterised by alternating marine and terrestrial facies and are associated with a mixture of different types of a source rock (kerogen type III and II) (e.g. Paterson & Mangerud, 2017). The Upper Triassic in the entire GBSB, particularly the De Geerdalen and Svenskøya formations (and their subsurface equivalents, the Snadd and Fruholmen Formations, respectively) are dominated by paralic and fluvio-deltaic facies. These deposits are characterised by the dominance of Type III kerogen (Paterson et al., 2017, 2019). The presence of thin coal beds in the Upper Triassic succession may represent an additional gas-prone source rock (Norina et al., 2014). The intervening Norian deposits, particularly the Flatsalen Formation and its subsurface equivalents in the northwest region, are typified by a high abundance of marine organic matter (Type II Kerogen) (Paterson et al., 2017, 2019). Flooding surfaces are regional and relatively good seals that well developed on a bigger part of the basin during the Lower and Middle Triassic. A local sealing mechanism for channelised deposits is likely to be overbank shales.

6 | CONCLUSIONS

This study presents a unified stratigraphic framework of the Triassic in the entire Greater Barents Sea Basin, which is a vast (1,200 × 1,800 km) intracratonic basin that includes the Southwestern and Northwestern Barents Sea, Svalbard, Eastern Barents Sea, Timan-Pechora Basin and North Kara Sea. The study is based on analysis of large amounts of seismic data in the region, all available well data and published information from outcrops of Triassic rocks in the region. These have been correlated using new palynological analyses from Russian wells presented herein, and published data for the entire GBSB. The majority of Triassic deposits in the GBSB consists of deposits of a low-gradient deltaic system including clinoformal prodelta mudstones, a mudstone rich deltaic topset and sandstone-dominated fluvial channels, that was fed from a 'continental-scale' catchment in Western Baltica, Urals and West Siberia. This system was active for

ca. 50 Myr (Induan to Rhaetian), and is characterised by sediment transport towards the northwest into the Greater Barents Sea Basin.

In the Lower Triassic, many of the flooding surfaces can be traced far into the Eastern parts of the Greater Barents Sea basin, but in the Middle and Late Triassic the sedimentary system progrades so far into the basin that marine flooding is not registered in the more proximal parts of the basin. Enormous amounts of sediments were supplied in the Early Triassic, lower sediment supply occurred during the Middle Triassic, and an increase in sediment supply is observed in the Carnian. These changes largely relate to tectonism in the source area, especially the onset of the Siberian Traps Large Igneous Province in the Early Triassic, relative tectonic quiescence in the Middle Triassic, and incipient uplift of the Novaya Zemlya and Pay-Khoy in the Late Triassic. Large amounts of sediment spilt over into adjacent basins throughout the Triassic in the North (towards the Lomonosov Ridge and possibly Chukchi Borderland) and during the Carnian and Norian towards the Atlantic Margin and Arctic Canada (Sverdrup basin) in the west and northwest, showing that provenance interpretations that require long-distance sediment transport across the GBSB to the wider arctic are reasonable. The results of this study can be used to guide petroleum exploration in the areas of the GBSB with little data because of how the different units correlate and how facies are developed within them. For example, channelised deposits in the distal part of the system well-positioned above the more prolific source rocks in front of the delta, and sandstones are likely better sorted compared to proximal equivalents. Furthermore, the great thickness of igneous intrusions in the Eastern Barents Sea Basin has to be taken into account when modelling basin subsidence and thickness of units.

ACKNOWLEDGEMENT

We acknowledge the Norwegian Research Council for funding through the Petromaks2-program to the ISBAR project (267689). We thank reviewers Atle Mørk, Owen Anfinson, Tony Doré and Steven Andrews for helpful suggestions that significantly improved this manuscript, and editor Cari Johnson for thorough editorial comments. We also thank William Helland-Hansen, Valentina Marzia Rossi, Hallgeir Sirevaag and Alice Newman for discussions and constructive comments on an early draft of this manuscript. PGS, TGS, MAGE, SMNG and the Norwegian Petroleum Directorate are acknowledged for providing seismic data and for permission to publish seismic lines. We also thank Schlumberger for providing software under educational licenses to the University of Bergen.

CONFLICTS OF INTEREST

The authors declare there are no conflicts of interest.

PEER REVIEW

The peer review history for this article is available at <https://publons.com/publon/10.1111/bre.12526>.

DATA AVAILABILITY STATEMENT

Some of the seismic reflection data are available from DISCOS dataset, other parts may be available upon request from the Norwegian Petroleum Directorate, PGS, TGS, MAGE and SMNG.

ORCID

Albina Gilmullina  <https://orcid.org/0000-0001-6187-9029>

Christian Haug Eide  <https://orcid.org/0000-0003-4949-9917>

REFERENCES

- Aarseth, I., Mjelde, R., Breivik, A. J., Minakov, A., Faleide, J. I., Flueh, E., & Huismans, R. S. (2017). Crustal structure and evolution of the Arctic Caledonides: Results from controlled-source seismology. *Tectonophysics*, *718*, 9–24. <https://doi.org/10.1016/j.tecto.2017.04.022>
- Abay, T. B., Karlsen, D. A., Pedersen, J. H., Olausen, S., & Backer-Owe, K. (2018). Thermal maturity, hydrocarbon potential and kerogen type of some Triassic-Lower Cretaceous sediments from the SW Barents Sea and Svalbard. *Petroleum Geoscience*, *24*(3), 349–373. <https://doi.org/10.1144/petgeo2017-035>
- Anfinson, O. A., Embry, A. F., & Stockli, D. F. (2016). Geochronologic constraints on the Permian-Triassic northern source region of the Sverdrup Basin, Canadian Arctic Islands. *Tectonophysics*, *691*, 206–219. <https://doi.org/10.1016/j.tecto.2016.02.041>
- Artyushkov, E. V., Belyaev, I. V., Kazanin, G. S., Pavlov, S. P., Chekhovich, P. A., & Shkarubo, S. I. (2014). Formation mechanisms of ultradeep sedimentary basins: The North Barents basin. Petroleum potential implications. *Russian Geology and Geophysics*, *55*(5), 649–667. <https://doi.org/10.1016/j.rgg.2014.05.009>
- Bergan, M., & Knarud, R. (1993). Apparent changes in clastic mineralogy of the Triassic-Jurassic succession, Norwegian Barents Sea: Possible implications for palaeodrainage and subsidence. In T. O. Vorren, E. Bergsager, & Ø. A. Dahl-Stammes (Eds.), *Norwegian Petroleum Society Special Publications* (Vol. 2, pp. 481–493). Elsevier.
- Bjærke, T., & Manum, S. B. (1977). Mesozoic palynology of Svalbard. I. The Rhaetian of Hopen, with a preliminary report on the Rhaetian and Jurassic of Kong Karls Land.
- Bjergager, M., Alsen, P., Hovikoski, J., Lindström, S., Pilgaard, A., Stemmerik, L., & Therkelsen, J. (2019). Triassic lithostratigraphy of the Wandel Sea Basin, North Greenland. *Bulletin of the Geological Society of Denmark*, *67*(1). <https://doi.org/10.37570/bgds-2019-67-06>
- Blum, M., & Pecha, M. (2014). Mid-Cretaceous to Paleocene North American drainage reorganisation from detrital zircons. *Geology*, *42*, 607–610.
- Blum, M. D., & Törnqvist, T. E. (2000). Fluvial responses to climate and sea-level change: A review and look forward. *Sedimentology*, *47*(s1), 2–48. <https://doi.org/10.1046/j.1365-3091.2000.00008.x>
- Buchan, K. L., & Ernst, R. E. (2018). A giant circumferential dyke swarm associated with the High Arctic Large Igneous Province

- (HALIP). *Gondwana Research*, 58, 39–57. <https://doi.org/10.1016/j.gr.2018.02.006>
- Bue, P. E., & Andresen, A. (2014). Constraining depositional models in the Barents Sea region using detrital zircon U-Pb data from Mesozoic sediments in Svalbard. *Geological Society, London, Special Publications*, 386(1), 261–279. <https://doi.org/10.1144/SP386.14>
- Burgess, S. D., & Bowering, S. A. (2015). High-precision geochronology confirms voluminous magmatism before, during, and after Earth's most severe extinction. *Science Advances*, 1(7), e1500470. <https://doi.org/10.1126/sciadv.1500470>
- Clark, S. A., Glorstad-Clark, E., Faleide, J. I., Schmid, D., Hartz, E. H., & Fjeldskaar, W. (2014). Southwest Barents Sea rift basin evolution: Comparing results from backstripping and time-forward modelling. *Basin Research*, 26(4), 550–566. <https://doi.org/10.1111/bre.12039>
- Cocks, L., & Torsvik, T. (2006). European geography in a global context from the Vendian to the end of the Palaeozoic. *Geological Society, London, Memoirs*, 32, 83. <https://doi.org/10.1144/GSL.MEM.2006.032.01.05>
- Cohen, K. M., Finney, S. C., Gibbard, P. L., & Fan, J.-X. (2013). The ICS international chronostratigraphic chart. *Episodes*, 36(3), 199–204. <https://doi.org/10.18814/epiiugs/2013/v36i3/002>
- Crameri, F. (2018). Geodynamic diagnostics, scientific visualisation and StagLab 3.0. *Geoscientific Model Development*, 11, 2541–2562. <https://doi.org/10.5194/gmd-11-2541-2018>
- Dalland, A., Worsley, D., & Ofstad, K. (1988). A lithostratigraphic scheme for the mesozoic and cenozoic and succession offshore mid- and northern Norway. Oljedirektoratet.
- Doré, A. G., Lundin, E. R., Gibbons, A., Sømme, T. O., & Tørudbakken, B. O. (2016). Transform margins of the Arctic: A synthesis and re-evaluation. *Geological Society, London, Special Publications*, 431(1), 63–94. <https://doi.org/10.1144/SP431.8>
- Doré, A. G., Lundin, E. R., Jensen, L. N., Birkeland, Ø., Eliassen, P. E., & Fichler, C. (1999, January). Principal tectonic events in the evolution of the northwest European Atlantic margin. In A. J. Fleet & S. A. R. Boldy (Eds.), *Geological Society, London, Petroleum Geology Conference Series* (Vol. 5(1), pp. 41–61). London: Geological Society.
- Drachev, S. S. (2016). Fold belts and sedimentary basins of the Eurasian Arctic. *Arktos*, 2, 21.
- Duran, E. R., di Primio, R., Anka, Z., Stoddart, D., & Horsfield, B. (2013). Petroleum system analysis of the Hammerfest Basin (southwestern Barents Sea): Comparison of basin modelling and geochemical data. *Organic geochemistry*, 63, 105–121.
- Dymov, V. A., Kachurina, N. V., Makaryev, A. A., Makaryeva, E. M., Orlov, V. V., & Stark, A. G. (2011). Gosudarstvennaya geologicheskaya karta Rossiyskoy Federatsii. Masshtab 1: 1 000 000 (tret'ye pokoleniye). Seriya Severo-Karsko-Barentsevomorskaya. List U-41-44 —Zemlya Frantsa-Iosifa (vostochnyye ostrova). Ob'yasnitel'naya zapiska.: 220.
- Dypvik, H., Sokolov, A., Pcelina, T., Fjellsa, B., Bjerke, T., Korchinskaya, M., & Nagy, J. (1998). The Triassic successions of Franz Josef Land, stratigraphy and sedimentology of three wells from Alexandra, Hayes and Graham-Bell islands. *Geological aspects of Franz Josef Land and the northernmost Barents Sea—the Northern Barents Sea Geotraverse. Norsk Polarinstittut Meddelelser*, 151, 50–82.
- Eide, C. H., Klausen, T. G., Katkov, D., Suslova, A. A., & Helland-Hansen, W. (2018). Linking an Early Triassic delta to antecedent topography: Source-to-sink study of the southwestern Barents Sea margin. *Bulletin*, 130(1–2), 263–283.
- Eide, C. H., Schofield, N., Jerram, D. A., & Howell, J. A. (2017). Basin-scale architecture of deeply emplaced sill complexes: Jameson Land, East Greenland. *Journal of the Geological Society*, 174(1), 23–40.
- Ershova, V. B., Prokopiev, A. V., Khudoley, A. K., Sobolev, N. N., & Petrov, E. O. (2015). U/Pb dating of detrital zircons from late Palaeozoic deposits of Bel'kovsky Island (New Siberian Islands): Critical testing of Arctic tectonic models. *International Geology Review*, 57(2), 199–210.
- Faleide, J. I., Gudlaugsson, S. T., & Jacquart, G. (1984). Evolution of the western Barents Sea. *Marine and Petroleum Geology*, 1(2), 123–150.
- Faleide, J. I., Tsikalas, F., Breivik, A. J., Mjelde, R., Ritzmann, O., Engen, O., Wilson, J., & Eldholm, O. (2008). Structure and evolution of the continental margin off Norway and the Barents Sea. *Episodes*, 31(1), 82–91.
- Fefilova, L. A. (2001). Miospory iz triasovykh otlozheniy tsentral'noy chasti o. Zapadnyy Shpitsbergen (Sassenf'ord, yuzhnoye poberezh'ye) (Triassic miospores from the central part of West Svalbard (Sassenfjord, south coast)). *Biostratigrafiya mezozoya i kaynozoya nekotorykh regionov Arktiki i Mirovogo okeana (Biostratigraphy of the Mesozoic and Cenozoic of some regions of the Arctic and the World Ocean)* (ed. VA Basov): 5–19.
- Fefilova, L. A. (2005). Palinokompleksy verkhnego Triasa Zemli Frantsa-Iosifa (Upper Triassic palynoassemblages of Franz-Josef Land). In S. A. Afonin, & P. I. Tokarev (Eds.), *XI vserossiyskaya palinologicheskaya konferentsiya "Palinologiya: teoriya i praktika"*, materia ly konferentsii 27 sentya brya – 1 oktyabrya 2005 (Proceedings of XI All-Russian palynological conference "Palynology: Theory & applications" 27 September – 1 October 2005) (pp. 266). PIN RAS. (In Russian with English summary).
- Fefilova, L. A. (2011). Palynological characteristic Rhaetian part of Triassic succession on Franz-Josef Land archipelago Problems of modern palynology: 13th Russian Palynological conference: 6.
- Fefilova, L. A. (2013a). Biostratigrafiya, miospory i makroflora triasovykh otlozheniy yugo-vostochnoy chasti shel'fa Barentseva moray na primere Krestovoy ploshchadi i soprodel'nykh rayonov (Biostratigraphy, miospores and macroflora of Triassic sediments of the southeastern part of the Barents Sea shelf on the example of Krestovaya Field and adjacent areas). *Scientific Materials on the biotratigraphy, fauna and flora of the Phanerozoic of Russia, the Atlantic and the Antarctic*, pp. 42–83. (In Russian).
- Fefilova, L. A. (2013b). Palinologicheskoye obosnovaniye nizhney granitsy triasovykh otlozheniy v razreze skv. Admiralteyskaya-1 (shel'f Barentseva moraya) (Palynological evidence on the Lower Triassic boundary in the Admiralteiskaya-1 well (the Barents Sea shelf)). *Scientific materials on the Phanerozoic biostratigraphy, fauna and flora from Russia, Atlantic and Antarctic*, pp. 84–97. (In Russian).
- Fefilova, L. A. (2015). New microfloristic data from the Permian and Triassic boundary sediments of the Russian Western Arctic (Novaya Zemlya archipelago and adjacent regions) // Paleobotanical temporary. Supplement to the magazine Lethaea rossica. - No. 2. - S. 229-240.
- Fleming, E. J., Flowerdew, M. J., Smyth, H. R., Scott, R. A., Morton, A. C., Omma, J. E., Frei, D., & Whitehouse, M. J. (2016). Provenance of Triassic sandstones on the southwest Barents Shelf and the implication for sediment dispersal patterns in northwest Pangaea. *Marine and Petroleum Geology*, 78, 516–535.

- Flowerdew, M. J., Fleming, E. J., Morton, A. C., Frei, D., Chew, D. M., & Daly, J. S. (2020). Assessing mineral fertility and bias in sedimentary provenance studies: Examples from the Barents Shelf. *Geological Society, London, Special Publications*, 484(1), 255–274.
- Francis, J. E. (1994). Palaeoclimates of Pangea—geological evidence. *Geological Society, London, Special Publications*, 484(1), 255–274.
- Friedrich, A. M., Bunge, H.-P., Rieger, S. M., Colli, L., Ghelichkhan, S., & Nerlich, R. (2018). Stratigraphic framework for the plume mode of mantle convection and the analysis of interregional unconformities on geological maps. *Gondwana Research*, 53, 159–188.
- Gabrielsen, R. H., Faereth, R. B., & Jensen, L. N. (1990). Structural elements of the Norwegian continental shelf. Pt. 1. The Barents Sea region. Norwegian Petroleum Directorate.
- Gac, S., Huisman, R. S., Podladchikov, Y. Y., & Faleide, J. I. (2012). On the origin of the ultradeep East Barents Sea basin. *Journal of Geophysical Research: Solid Earth*, 117(B4).
- Gac, S., Huisman, R. S., Simon, N. S., Faleide, J. I., & Podladchikov, Y. Y. (2014). Effects of lithosphere buckling on subsidence and hydrocarbon maturation: A case-study from the ultra-deep East Barents Sea basin. *Earth and Planetary Science Letters*, 407, 123–133.
- Galloway, W. E., Whiteaker, T. L., & Ganey-Curry, P. (2011). History of Cenozoic North American drainage basin evolution, sediment yield, and accumulation in the Gulf of Mexico basin. *Geosphere*, 7(4), 938–973.
- Gardiner, D., Schofield, N., Finlay, A., Mark, N., Holt, L., Grove, C., Forster, C., & Moore, J. (2019). Modeling petroleum expulsion in sedimentary basins: The importance of igneous intrusion timing and basement composition. *Geology*, 47(10), 904–908. <https://doi.org/10.1130/G46578.1>
- Gavrilov, V. P., Tibshman, N. B., Karnaukhov, S. M., Holodilov, V. L., Tsemkalo, M. L., & Shamalov Y. V. (2010). *Biostratigrafiya i litofatsiya neftegazonosnykh otlozheniy Barentsevo-Karskogo regiona. (Biostratigraphy and lithofacies of oil and gas deposits in the Barents-Kara region)*. - M.: Nedra Publishing House LLC. 255 p.: ill. (In Russian).
- Glørstad-Clark, E., Faleide, J. I., Lundschie, B. A., & Nystuen, J. P. (2010). Triassic seismic sequence stratigraphy and paleogeography of the western Barents Sea area. *Marine and Petroleum Geology*, 27(7), 1448–1475. <https://doi.org/10.1016/j.marpetgeo.2010.02.008>
- Gradstein, F. M., Ogg, J. G., Schmitz, M., & Ogg, G. M. (2012). *The geologic time scale 2012*. Elsevier.
- Grantz, A., Pease, V. L., Willard, D. A., Phillips, R. L., & Clark, D. L. (2001). Bedrock cores from 89° North: Implications for the geologic framework and Neogene paleoceanography of Lomonosov Ridge and a tie to the Barents shelf. *Geological Society of America Bulletin*, 113(10), 1272–1281. [https://doi.org/10.1130/0016-7606\(2001\)113%3C1272:BCFNIF%3E2.0.CO;2](https://doi.org/10.1130/0016-7606(2001)113%3C1272:BCFNIF%3E2.0.CO;2)
- Gudlaugsson, S. T., Faleide, J. I., Johansen, S. E., & Breivik, A. J. (1998). Late Palaeozoic structural development of the South-western Barents Sea. *Marine and Petroleum Geology*, 15(1), 73–102. [https://doi.org/10.1016/S0264-8172\(97\)00048-2](https://doi.org/10.1016/S0264-8172(97)00048-2)
- Haile, B. G., Klausen, T. G., Jähren, J., Braathen, A., & Hellevang, H. (2018). Thermal history of a Triassic sedimentary sequence verified by a multi-method approach: Edgeøya, Svalbard. Norway. *Basin Research*, 30(6), 1075–1097. <https://doi.org/10.1111/bre.12292>
- Helland-Hansen, W., Sømme, T. O., Martinsen, O. J., Lunt, I., & Thurmond, J. (2016). Deciphering Earth's natural hourglasses: Perspectives on source-to-sink analysis. *Journal of Sedimentary Research*, 86(9), 1008–1033. <https://doi.org/10.2110/jsr.2016.56>
- Henriksen, E., Bjørnseth, H. M., Hals, T. K., Heide, T., Kiryukhina, T., Kløvjan, O. S., Larssen, G. B., Ryseth, A. E., Rønning, K., Sollid, K., & Stoupakova, A. (2011). Uplift and erosion of the greater Barents Sea: Impact on prospectivity and petroleum systems. *Geological Society, London, Memoirs*, 35(1), 271–281.
- Henriksen, E., Ryseth, A., Larssen, G. B., Heide, T., Rønning, K., Sollid, K., & Stoupakova, A. V. (2011). Chapter 10: Tectonostratigraphy of the greater Barents Sea: Implications for petroleum systems. *Geological Society, London, Memoirs*, 35(1), 163–195.
- Henriksen, T., & Ulfstein, G. (2011). Maritime Delimitation in the Arctic: The Barents Sea Treaty. *Ocean Development & International Law*, 42(1–2), 1–21. <https://doi.org/10.1080/00908320.2011.542389>
- Hermann, E., Hochuli, P. A., Bucher, H., Vigran, J. O., Weissert, H., & Bernasconi, S. M. (2010). A close-up view of the Permian-Triassic boundary based on expanded organic carbon isotope records from Norway (Trøndelag and Finnmark Platform). *Global and Planetary Change*, 74(3–4), 156–167. <https://doi.org/10.1016/j.gloplacha.2010.10.007>
- Hochuli, P., Colin, J., & Vigran, J. O. (1989). *Triassic biostratigraphy of the Barents Sea area. Correlation in hydrocarbon exploration* (pp. 131–153). Springer.
- Ivanova, N. M., Sakulina, T. S., Belyaev, I. V., Matveev, Y. I., & Roslov, Y. V. (2011). Chapter 12 Depth model of the Barents and Kara seas according to geophysical surveys results. *Geological Society, London, Memoirs*, 35(1), 209–221.
- Jarsve, E. M., Maast, T. E., Gabrielsen, R. H., Faleide, J. I., Nystuen, J. P., & Sassier, C. (2014). Seismic stratigraphic subdivision of the Triassic succession in the Central North Sea; integrating seismic reflection and well data. *Journal of the Geological Society*, 171(3), 353–374. <https://doi.org/10.1144/jgs2013-056>
- Kirichkova, A. I., & Esenina, A. V. (2016). Pteridospermovye (pino-phyta) Middle Triassic Timan-Pechora Basin // Stratigraphy. Geological correlation. T. 24. - No. 2. - S. 17–17.
- Klausen, T. G., & Mørk, A. (2014). The Upper Triassic paralic deposits of the De Geerdalen Formation on Hopen: Outcrop analog to the subsurface Snadd Formation in the Barents Sea The De Geerdalen Formation on Hopen. *AAPG Bulletin*, 98(10), 1911–1941. <https://doi.org/10.1306/02191413064>
- Klausen, T. G., Nyberg, B., & Helland-Hansen, W. (2019). The largest delta plain in Earth's history. *Geology*, 47(5), 470–474. <https://doi.org/10.1130/G45507.1>
- Klausen, T. G., Ryseth, A. E., Helland-Hansen, W., Gawthorpe, R., & Laursen, I. (2014). Spatial and temporal changes in geometries of fluvial channel bodies from the Triassic Snadd Formation of offshore Norway. *Journal of Sedimentary Research*, 84(7), 567–585. <https://doi.org/10.2110/jsr.2014.47>
- Klausen, T. G., Ryseth, A. E., Helland-Hansen, W., Gawthorpe, R., & Laursen, I. (2015). Regional development and sequence stratigraphy of the Middle to Late Triassic Snadd formation, Norwegian Barents Sea. *Marine and Petroleum Geology*, 62, 102–122. <https://doi.org/10.1016/j.marpetgeo.2015.02.004>
- Klausen, T. G., Ryseth, A., Helland-Hansen, W., & Gjelberg, H. K. (2016). Progradational and backstepping shoreface deposits in the Ladinian to Early Norian Snadd Formation of the Barents Sea. *Sedimentology*, 63(4), 893–916. <https://doi.org/10.1111/sed.12242>
- Klausen, T. G., Torland, J. A., Eide, C. H., Alaei, B., Olausen, S., & Chiarella, D. (2018). Cliniform development and topset evolution in a mud-rich delta – The Middle Triassic Kobbe Formation, Norwegian Barents Sea. *Sedimentology*, 65(4), 1132–1169. <https://doi.org/10.1111/sed.12417>

- Klubov, B. (1965). Triassic and Jurassic deposits of Wilhelm Island. *Data on the geology of the Spitsbergen. Leningrad, Nauchno-issledovatel'skiy institut geologii Arctiki*: 174–184.
- Korchinskaya, M. V., & Semevskij, D. V. (1980). Rannenorijskaja fauna archipelaga Sval'bard.(Early Norian fauna of the archipelago of Svalbard.) //Geologija osadoč nogo č echla archipelaga Sval'bard.(Geology of the sedimentary platform cover of the archipelago of Svalbard.): Leningrad, NIIGA. C. 30–43.
- Krajewski, K., & Weitschat, W. (2015). Depositional history of the youngest strata of the Sassendalen Group (Bravaisberget Formation, Middle Triassic–Carnian) in southern Spitsbergen, Svalbard. *Annales Societatis Geologorum Poloniae*, 85, 151–175. <https://doi.org/10.14241/asgp.2014.005>
- Leith, T., Weiss, H., Mørk, A., Elvebakk, G., Embry, A. F., Brooks, P. W., Stewart, K. R., Pchelina, T. M., Bro, E. G., Verba, M. L., & Danyushevskaya, A. (1993). Mesozoic hydrocarbon source-rocks of the Arctic region. In T. O. Vorren, E. Bergsager, Ø. A. Dahl-Stamnes, E. Holter, B. Johansen, E. Lie, & T. B. Lund (Eds.), *Norwegian Petroleum Society Special Publications* (Vol. 2, pp. 1–25). Elsevier.
- Lord, G. S., Mørk, M. B. E., Mørk, A., & Olaussen, S. (2019). Sedimentology and petrography of the Svenskøya Formation on Hopen, Svalbard: An analogue to sandstone reservoirs in the Realgrunnen Subgroup. *Polar Research*, 38. <https://doi.org/10.33265/polar.v38.3523>
- Lord, G. S., Solvi, K. H., Klausen, T. G., Mørk, A. (2014). Triassic channel bodies on Hopen, Svalbard: Their facies, stratigraphical significance and spatial distribution. *Norwegian Petroleum Directorate Bulletin*, 11, 41–59.
- Lundschien, B. A., Høy, T., & Mørk, A. (2014). Triassic hydrocarbon potential in the Northern Barents Sea; integrating Svalbard and stratigraphic core data. *Norwegian Petroleum Directorate Bulletin*, 11(11), 3–20.
- Mark, N., Schofield, N., Gardiner, D., Holt, L., Grove, C., Watson, D., Alexander, A., & Poore, H. (2019). Overthickening of sedimentary sequences by igneous intrusions. *Journal of the Geological Society*, 176(1), 46–60. <https://doi.org/10.1144/jgs2018-112>
- Martin, J., Fernandes, A. M., Pickering, J., Howes, N., Mann, S., & McNeil, K. (2018). The stratigraphically preserved signature of persistent backwater dynamics in a large paleodelta system: The Mungaroo Formation, North West Shelf. *Australia. Journal of Sedimentary Research*, 88(7), 850–872.
- Miller, E. L., Meisling, K. E., Akinin, V. V., Brumley, K., Coakley, B. J., Gottlieb, E. S., Hoiland, C. W., O'Brien, T. M., Soboleva, A., & Toro, J. (2018). Circum-Arctic Lithosphere Evolution (CALE) Transect C: Displacement of the Arctic Alaska-Chukotka microplate towards the Pacific during opening of the Amerasia Basin of the Arctic. *Geological Society, London, Special Publications*, 460(1), 57.
- Miller, E. L., Soloviev, A. V., Prokopiev, A. V., Toro, J., Harris, D., Kuzmichev, A. B., & Gehrels, G. E. (2013). Triassic river systems and the paleo-Pacific margin of northwestern Pangea. *Gondwana Research*, 23(4), 1631–1645.
- Minakov, A., Yarushina, V., Faleide, J. I., Krupnova, N., Sakoulina, T., Dergunov, N., & Glebovsky, V. (2018). Dyke emplacement and crustal structure within a continental large igneous province, northern Barents Sea. *Geological Society, London, Special Publications*, 460(1), 371–395.
- Morakhovskaja, E. D. (2000). Triassic deposits of Timan-Ural region (key sections, stratigraphy, correlation). *Biochronology and Correlation of Phanerozoic of Oil and Gas Basins of the Russia*, 1, 80.
- Mørk, A., Dallmann, W. K., Dypvik, H., Johannessen, E. P., Larssen, G. B., Nagy, J., Nøttvedt, A., Olaussen, S., Pchelina, T. M., & Worsley, D. (1999). Mesozoic lithostratigraphy. In W. K. Dallmann (Ed.), *Lithostratigraphic lexicon of Svalbard. Upper Palaeozoic to Quaternary bedrock. Review and recommendations for nomenclature use* (pp. 127–214). Tromsø: Norsk Polarinstitutt.
- Mørk, A., Elvebakk, G., Forsberg, A. W., Hounslow, M. W., Nakrem, H. A., Vigran, J. O., & Weitschat, W. (1999). The type section of the Vikinghogda Formation: A new Lower Triassic unit in central and eastern Svalbard. *Polar Research*, 18(1), 51–82.
- Mørk, A., Embry, A. F., & Weitschat, W. (1989). *Triassic transgressive-regressive cycles in the Sverdrup Basin, Svalbard and the Barents Shelf. Correlation in hydrocarbon exploration* (pp. 113–130). Springer.
- Mørk, A., Vigran, J., Korchinskaya, M., Pchelina, T. M., Fefilova, L. A., Vavilov, M. N., & Weitschat, W. (1993). Triassic rocks in Svalbard, the Arctic Soviet islands and the Barents Shelf: Bearing on their correlations. In *Norwegian Petroleum Society Special Publications* (Vol. 2, pp. 457–479). Elsevier.
- Mørk, A., & Worsley, D. (2006). Triassic of Svalbard and the Barents shelf. *NGF Abstracts and Proceedings*, 3, 23–29.
- Mørk, M. B. E. (1999). Compositional variations and provenance of Triassic sandstones from the Barents Shelf. *Journal of Sedimentary Research*, 69(3), 690–710. <https://doi.org/10.2110/jsr.69.690>
- Mueller, S., Hounslow, M. W., & Kürschner, W. M. (2016). Integrated stratigraphy and palaeoclimate history of the Carnian Pluvial Event in the Boreal realm; new data from the Upper Triassic Kapp Toscana Group in central Spitsbergen (Norway). *Journal of the Geological Society*, 173(1), 186–202.
- Müller, R., Klausen, T. G., Faleide, J. I., Olaussen, S., Eide, C. H., & Suslova, A. (2019). Linking regional unconformities in the Barents Sea to compression-induced forebulge uplift at the Triassic-Jurassic transition. *Tectonophysics*, 765, 35–51.
- Nikishin, A. M., Petrov, E. I., Cloetingh, S., Freiman, S. I., Malyshev, N. A., Morozov, A. F., Posamentier, H. W., Verzhbitsky, V. E., Zhukov, N. N., & Startseva, K. (2019). Geological structure and history of the Arctic Ocean based on new geophysical data: Implications for paleoenvironment and paleoclimate. Part 2. Mesozoic to Cenozoic geological evolution. *Earth-Science Reviews*, 103034. <https://doi.org/10.1016/j.earscirev.2019.103034>
- Nikishin, A. M., Petrov, E. I., Malyshev, N. A., & Ershova, V. P. (2017). Rift systems of the Russian Eastern Arctic shelf and Arctic deep water basins: Link between geological history and geodynamics. *Geodynamics & Tectonophysics*, 8, 11–43. <https://doi.org/10.5800/GT-2017-8-1-0231>
- Nikishin, A. M., Sobornov, K. O., Prokopiev, A. V., & Frolov, S. V. (2010). Tectonic evolution of the Siberian Platform during the Vendian and Phanerozoic. *Moscow University Geology Bulletin*, 65(1), 1–16.
- Nikishin, A. M., Ziegler, P. A., Abbott, D., Brunet, M. F., & Cloetingh, S. A. P. L. (2002). Permo-Triassic intraplate magmatism and rifting in Eurasia: Implications for mantle plumes and mantle dynamics. *Tectonophysics*, 351(1–2), 3–39.
- Norina, D. A., Stupakova, A. V., & Kiryukhina, T. A. (2014). Depositional environments and the hydrocarbon generative potential of Triassic rocks of the Barents Sea Basin. *Moscow University Geology Bulletin*, 69, 1–10. <https://doi.org/10.3103/S0145875214010062>
- Nyberg, B., & Howell, J. A. (2015). Is the present the key to the past? A global characterisation of modern sedimentary basins. *Geology*, 43(7), 643–646.

- Ogg, J. G., Huang, C., & Hinnov, L. (2014). Triassic timescale status: A brief overview. *Albertiana*, 41, 3–30.
- Olaussen, S., Larssen, G. B., Helland-Hansen, W., Johannessen, E. P., Nøttvedt, A., Riis, F., Rismyhr, B., Smelror, M., & Worsley, D. (2018). Mesozoic strata of Kong Karls Land, Svalbard, Norway; a link to the northern Barents Sea basins and platforms. *Norwegian Journal of Geology/Norsk Geologisk Forening*, 98(4). <https://doi.org/10.17850/njg98-4-06>
- Paterson, N. W., & Mangerud, G. (2015). Late Triassic (Carnian – Rhaetian) palynology of Hopen, Svalbard. *Review of Palaeobotany and Palynology*, 220, 98–119.
- Paterson, N. W., & Mangerud, G. (2017). Palynology and depositional environments of the Middle – Late Triassic (Anisian – Rhaetian) Kobbe, Snadd and Fruholmen formations, southern Barents Sea, Arctic Norway. *Marine and Petroleum Geology*, 86, 304–324. <https://doi.org/10.1016/j.marpetgeo.2017.05.033>
- Paterson, N. W., & Mangerud, G. (2020). A revised palynozonation for the Middle-Upper Triassic (Anisian–Rhaetian) Series of the Norwegian Arctic. *Geological Magazine*, 157(10), 1568–1592. <https://doi.org/10.1017/S0016756819000906>
- Paterson, N. W., Mangerud, G., Holen, L. H., Landa, J., Lundschieen, B. A., & Eide, F. (2019). Late Triassic (early Carnian–Norian) palynology of the Sentralbanken High, Norwegian Barents Sea. *Palynology*, 43(1), 53–75. <https://doi.org/10.1080/01916122.2017.1413018>
- Paterson, N. W., Mangerud, G., & Mørk, A. (2017). Late Triassic (early Carnian) palynology of shallow stratigraphical core 7830/5-U-1, offshore Kong Karls Land, Norwegian Arctic. *Palynology*, 41(2), 230–254.
- Pease, V., Drachev, S., Stephenson, R., & Zhang, X. (2014). Arctic lithosphere—A review. *Tectonophysics*, 628, 1–25. <https://doi.org/10.1016/j.tecto.2014.05.033>
- Plint, A. G., Tyagi, A., Hay, M. J., Varban, B. L., Zhang, H., & Roca, X. (2009). Clinoforms, paleobathymetry, and mud dispersal across the Western Canada Cretaceous foreland basin: Evidence from the Cenomanian Dunvegan Formation and contiguous strata. *Journal of Sedimentary Research*, 79(3), 144–161. <https://doi.org/10.2110/jsr.2009.020>
- Polteau, S., Hendriks, B. W. H., Planke, S., Ganerød, M., Corfu, F., Faleide, J. I., Midtkandal, I., Svendsen, H. S., & Myklebust, R. (2016). The Early Cretaceous Barents Sea Sill Complex: Distribution, 40Ar/39Ar geochronology, and implications for carbon gas formation. *Palaeogeography, Palaeoclimatology, Palaeoecology*, 441, 83–95. <https://doi.org/10.1016/j.palaeo.2015.07.007>
- Puchkov, V. N. (2009). The evolution of the Uralian orogen. *Geological Society, London, Special Publications*, 327(1), 161–195. <https://doi.org/10.1144/SP327.9>
- Puchkov, V. N. (2010). Geology of the Urals and Cis-Urals (actual problems of stratigraphy, tectonics, geodynamics and metallogeny). 280.
- Reichow, M. K., Pringle, M. S., Al'Mukhamedov, A. I., Allen, M. B., Andreichev, V. L., Buslov, M. M., Davies, C. E., Fedoseev, G. S., Fitton, J. G., Inger, S., Medvedev, A. Y., Mitchell, C., Puchkov, V. N., Safonova, I. Y., Scott, R. A., & Saunders, A. D. (2009). The timing and extent of the eruption of the Siberian Traps large igneous province: Implications for the end-Permian environmental crisis. *Earth and Planetary Science Letters*, 277(1), 9–20. <https://doi.org/10.1016/j.epsl.2008.09.030>
- Repin, Y. S., Fedorova, A. A., Bystrova, V. V., Kulikova, N. A., & Polubotko, I. V. (2007). Mesozoic of the Barents Sea sedimentation basin // Stratigraphy and its role in the development of the oil and gas complex of Russia. SPb., VNIGRI.– S. 112–161.
- Resource report. (2016). https://www.npd.no/globalassets/1-ncpd/publi_kasjoner/ressursrapporter-arkiv/resource-report-2016.pdf
- Resource report. (2017). https://www.npd.no/globalassets/1-ncpd/publi_kasjoner/rapporter-en/geologivurderingbhn-engelsk-lavoppl.pdf
- Riis, F., Lundschieen, B. A., Høy, T., Mørk, A., & Mørk, M. B. E. (2008). Evolution of the Triassic shelf in the northern Barents Sea region. *Polar Research*, 27(3), 318–338. <https://doi.org/10.1111/j.1751-8369.2008.00086.x>
- Rojo, L. A., Cardozo, N., Escalona, A., & Koyi, H. (2019). Structural style and evolution of the Nordkapp Basin, Norwegian Barents Sea. *AAPG Bulletin*, 103, 2177–2217.
- Rossi, V. M., Paterson, N. W., Helland-Hansen, W., Klausen, T. G., & Eide, C. H. (2019). Mud-rich delta-scale compound clinoforms in the Triassic shelf of northern Pangea (Havert Formation, southwestern Barents Sea). *Sedimentology*, 66(6), 2234–2267.
- Ruffell, A., Simms, M., & Wignall, P. (2016). The Carnian Humid Episode of the late Triassic: A review. *Geological Magazine*, 153(2), 271–284.
- Schofield, N., Heaton, L., Holford, S. P., Archer, S. G., Jackson, C. A., & Jolley, D. W. (2012). Seismic imaging of ‘broken bridges’: Linking seismic to outcrop-scale investigations of intrusive magma lobes. *Journal of the Geological Society*, 169(4), 421–426.
- Scotese, C. R., & Wright, N. (2018). PALEOMAP paleodigital elevation models (PaleoDEMS) for the Phanerozoic. <https://www.earthbyte.org/paleodem-resource-scotese-and-wright-2018>
- Scott, R. A., Howard, J. P., Guo, L., Schekoldin, R., & Pease, V. (2010, January). Offset and curvature of the Novaya Zemlya fold-and-thrust belt, Arctic Russia. In B. A. Vining & S. C. Pickering (Eds.), *Geological Society, London, Petroleum Geology Conference Series* (Vol. 7(1), pp. 645–657). London: Geological Society.
- Seton, M., Müller, R. D., Zahirovic, S., Gaina, C., Torsvik, T., Shephard, G., Talsma, A., Gurnis, M., Turner, M., Maus, S., & Chandler, M. (2012). Global continental and ocean basin reconstructions since 200Ma. *Earth-Science Reviews*, 113(3), 212–270.
- Shephard, G., Müller, D., & Seton, M. (2013). The tectonic evolution of the Arctic since Pangea breakup: Integrating constraints from surface geology and geophysics with mantle structure. *Earth-Science Reviews*, 124, 148–183.
- Simms, M. J., & Ruffell, A. H. (1989). Synchronicity of climatic change and extinctions in the Late Triassic. *Geology*, 17(3), 265–268.
- Smelror, M., Larssen, G. B., Olaussen, S., Rømuld, A., & Williams, R. (2019). Late Triassic to Early Cretaceous palynostratigraphy of Kong Karls Land, Svalbard, Arctic Norway, with correlations to Franz Josef Land, Arctic Russia. *Norwegian Journal of Geology*, 98(4), 1–31. <https://doi.org/10.17850/njg004>
- Smith, D. G. (1982). Stratigraphic significance of a palynoflora from ammonoidbearing Early Norian strata in Svalbard. *Newsletters on Stratigraphy*, 11(3), 154–161.
- Smith, D. G., Harland, W., & Hughes, N. (1975). Geology of Hopen, Svalbard. *Geological Magazine*, 112(1), 1–23. <https://doi.org/10.1017/S0016756800045544>
- Sobolev, A. V., Sobolev, S. V., Kuzmin, D. V., Malitch, K. N., & Petrulin, A. G. (2009). Siberian meimechites: Origin and relation to flood basalts and kimberliteS. *Geology and Geophysics*, 50(12), 1293–1334. <https://doi.org/10.1016/j.rgg.2009.11.002>
- Sømme, T. O., Doré, A. G., Lundin, E. R., & Tørudbakken, B. O. (2018). Triassic-Paleogene paleogeography of the Arctic: Implications for sediment routing and basin fill. *AAPG Bulletin*, 102, 2481–2517. <https://doi.org/10.1306/05111817254>

- Stoupakova, A. V. (2001). Development of sedimentary basins of an ancient continental margin and their oil-gas potential (in example of Barents Sea shelf). *Petroleum Geology*, 35, 49.
- Stoupakova, A. V. (2011). Structure and petroleum potential of the Barents-Kara Shelf and adjacent territories. *Oil and Gas Geology*, 6, 99–115.
- Stoupakova, A. V., Henriksen, E., Burlin, Y. K., Larsen, G. B., Milne, J. K., Kiryukhina, T. A., Golynchik, P. O., Bordunov, S. I., Ogarkova, M. P., & Suslova, A. A. (2011). The geological evolution and hydrocarbon potential of the Barents and Kara shelves. *Geological Society, London, Memoirs*, 35, 325–344. <https://doi.org/10.1144/M35.21>
- Suslova, A. A. (2014). Seismostratigraphic analysis and prospects of Jurassic Deposits, Barents Sea Shelf. *Petroleum Geology - Theoretical and Applied Studies*, 9(2), 1–19.
- Toporkov, V. G., & Denisenko, A. S. (2008). Prakticheskoye Primeneniye Dannya Yamr Dlya Otsenki Svoystv I Struktury Porod Produktivnykh Neftegazonosnykh Zalezhey. *Каротажник*, 12, 162–188.
- Traverse, A. (2007). *Paleopalynology*. Springer Science & Business Media.
- Ustritsky, V. I. (1981). Triassic and Upper Permian deposits of the Admiralty Peninsula (Novaya Zemlya) // Lithology and paleogeography of the Barents and Kara Seas. L.: NIIGA. - S. 55–65.
- Ustritsky, V. I., & Tugarova, M. A. (2013). Unique section of the Permian and Triassic, discovered by the Admiralteyskaya-1 well (Barents Sea) // Oil and gas geology. Theory and practice. - T. 8. - No. 2. - S. 1–1.
- Vigran, J. O., Mangerud, G., Mørk, A., Worsley, D., & Hochuli, P. A. (2014). *Palynology and geology of the Triassic succession of Svalbard and the Barents Sea* (Vol. 14). Norges geologiske undersøkelse.
- Vigran, J. O., Mangerud, G., Mørk, A., Bugge, T., & Weitschat, W. (1998). Biostratigraphy and sequence stratigraphy of the Lower and Middle Triassic deposits from the Svalis Dome, Central Barents Sea, Norway. *Palynology*, 22, 89–141. <https://doi.org/10.1080/01916122.1998.9989505>
- Vigran, J. O., Mørk, A., Forsberg, A. W., Weiss, H. M., & Weitschat, W. (2008). Tasmanites algae—Contributors to the Middle Triassic hydrocarbon source rocks of Svalbard and the Barents Shelf. *Polar Research*, 27(3), 360–371.
- Viskunova, K. G., Zinchenko, A. G., Kiiko, O. A., Kozlov, O. A., Kostin, D. A., Musatov, E. E., Pavlenkin, A. D., Povysheva, L. G., Preobrazhenskaya, E. N., Ustinov, N. V., Shipilov, E. V., Shkarubo, S. I., & Yakovleva, T. (2000). Ob'yasnitel'naya zapiska. Gosudarstvennaya geologicheskaya karta Rossiyskoy Federatsii. Masshtab 1:1000 000. (novaya seriya). (Explanatory letter. State geological map of the Russian Federation. Scale 1: 1,000,000. (New series)). List S- (36), 37 - Barents Sea - VSEGEI SPb, 2000.– 165 p. (In Russian).
- Wignall, P. B. (2001). Large igneous provinces and mass extinctions. *Earth-science Reviews*, 53(1–2), 1–33. [https://doi.org/10.1016/S0012-8252\(00\)00037-4](https://doi.org/10.1016/S0012-8252(00)00037-4)
- Worsley, D. (2008). The post-Caledonian development of Svalbard and the western Barents Sea. *Polar Research*, 27(3), 298–317. <https://doi.org/10.1111/j.1751-8369.2008.00085.x>
- Xu, G., Hannah, J. L., Stein, H. J., Mørk, A., Vigran, J. O., Bingen, B., Schutt, D. L., & Lundschie, B. A. (2014). Cause of Upper Triassic climate crisis revealed by Re–Os geochemistry of Boreal black shales. *Palaeogeography, Palaeoclimatology, Palaeoecology*, 395, 222–232. <https://doi.org/10.1016/j.palaeo.2013.12.027>
- Zhang, X., Pease, V., Carter, A., & Scott, R. (2018). Reconstructing Palaeozoic and Mesozoic tectonic evolution of Novaya Zemlya: combining geochronology and thermochronology. *Geological Society, London, Special Publications*, 460(1), 335–353.

SUPPORTING INFORMATION

Additional Supporting Information may be found online in the Supporting Information section.

How to cite this article: Gilmullina A, Klausen TG, Paterson NW, Suslova A, Eide CH. Regional correlation and seismic stratigraphy of Triassic Strata in the Greater Barents Sea: Implications for sediment transport in Arctic basins. *Basin Res.* 2021;33:1546–1579. <https://doi.org/10.1111/bre.12526>